Azimuthal asymmetries for hadron distributions inside a jet in hadronic collisions

Umberto D'Alesio,[1,2,*] Francesco Murgia,[2,†] and Cristian Pisano[1,2,‡]

[1]*Dipartimento di Fisica, Università di Cagliari, Cittadella Universitaria, I-09042 Monserrato (CA), Italy*
[2]*Istituto Nazionale di Fisica Nucleare, Sezione di Cagliari, C. P. 170, I-09042 Monserrato (CA), Italy*

(Received 23 November 2010; published 17 February 2011)

Using a generalized parton model approach including spin and intrinsic parton motion effects, and assuming the validity of factorization for large-p_T jet production in hadronic collisions, we study the azimuthal distribution around the jet axis of leading unpolarized or (pseudo)scalar hadrons, namely pions, produced in the jet fragmentation process. We identify the observable leading-twist azimuthal asymmetries for the unpolarized and single-polarized case related to quark and gluon-originated jets. We account for all physically allowed combinations of the transverse momentum–dependent (TMD) parton distribution and fragmentation functions, with special attention to the Sivers, Boer-Mulders, and transversity quark distributions, and to the Collins fragmentation function for quarks (and to the analogous functions for gluons). For each of these effects we evaluate, at central and forward rapidities and for kinematical configurations accessible at BNL-RHIC, the corresponding potentially maximized asymmetry (for π^+ production), obtained by saturating natural positivity bounds (and the Soffer bound for transversity) for the distribution and fragmentation functions involved and summing additively all partonic contributions. We then estimate, for both neutral and charged pions, the asymmetries involving TMD functions for which parametrizations are available. We also study the role of the different mechanisms, and the corresponding transverse single-spin asymmetries, for large-p_T inclusive-jet production.

DOI: 10.1103/PhysRevD.83.034021 PACS numbers: 13.88.+e, 12.38.Bx, 13.85.Ni, 13.87.Fh

I. INTRODUCTION

Transverse single-spin and azimuthal asymmetries in high-energy hadronic reactions have raised a lot of interest in the last years (see, e.g., Refs. [1,2] and references therein). Huge spin asymmetries have been measured in the inclusive forward production of pions in high-energy pp collisions at moderately large transverse momentum. The general trend of the early pioneer measurements of the E704 Collaboration at Fermilab [3,4] has been recently confirmed at much larger center-of-mass (c.m.) energies at the Relativistic Heavy Ion Collider (RHIC) at Brookhaven National Laboratories (BNL) in similar kinematical configurations [5,6]. A surprisingly large transverse polarization of Λ hyperons produced in the forward region was also measured in unpolarized pp, pN fixed-target experiments (see, e.g., Ref. [7]). In this case, too, it will hopefully be possible in the near future to check if this intriguing effect survives at the much larger energies reachable at RHIC and at the Large Hadron Collider (LHC) at CERN. Similar effects, leading to azimuthal asymmetries both in the polarized and unpolarized case, have been measured in Drell-Yan (DY) processes [8,9], in semi-inclusive deeply inelastic scattering (SIDIS) [10–13], and in hadron-pair production in e^+e^- collisions [14,15].

These results cannot be explained at leading-twist (LT) approximation in the usual collinear approach of perturbative QCD (pQCD), based on factorization theorems, to inclusive particle production in hadronic collisions. Here collinear means that intrinsic parton motion is neglected in the hard scattering processes and integrated over up to the large energy scale in the soft functions involved. On the contrary, at least in the kinematical regimes under consideration at RHIC, collinear next-to-leading order (NLO) pQCD gives a fair account of unpolarized cross sections (see, e.g., Refs. [16,17]).

Two different main theoretical approaches have been proposed in the framework of perturbative QCD in order to account for these measurements. One is the so-called twist-three collinear approach, which generalizes the leading-order (LO) collinear framework with the inclusion of higher-twist quark-gluon correlations [18–20]. This involves a new class of universal nonperturbative twist-three quark-gluon distribution and fragmentation functions that need to be modeled by fitting experimental data. Another formalism, which will be adopted in this paper, is the so-called transverse momentum–dependent (TMD) approach, which takes into account spin and intrinsic parton motion effects.

Although the large single-spin asymmetries (SSAs) of interest here were originally observed in single inclusive particle production in hadronic collisions, it is now clear that from the theoretical point of view these are not the cleanest processes to consider. First of all, these SSAs are twist-three effects in a series expansion in inverse powers of the large energy scale (here, the transverse momentum of the observed single hadron or jet). Several competing mechanisms can therefore play a role and mix up. Moreover, in the TMD formalism factorization has not yet

*umberto.dalesio@ca.infn.it
†francesco.murgia@ca.infn.it
‡cristian.pisano@ca.infn.it

been proven for these processes and its validity is presently under much debate; see, e.g., Refs. [21] for inclusive one-hadron production and [22–27] for inclusive two-hadron production. Factorization breaking would in turn imply nonuniversality of the soft TMD distribution and fragmentation functions required to explain data. In the case of single particle production in hadronic collisions, therefore, the TMD approach can be seen at present as a useful generalization of the parton model where factorization is assumed as a reasonable starting point to be carefully scrutinized by comparison with available experimental results.

As mentioned above, similar spin and azimuthal asymmetries were subsequently observed in SIDIS and DY processes, where two energy scales are involved, the required large energy scale (the momentum transfer Q in SIDIS, the lepton-pair invariant mass, M, in DY) allowing use of pQCD, and a small energy scale sensitive to intrinsic parton motion (the transverse momentum, respectively, of the final lepton pair in DY and of the produced hadron in SIDIS). For these classes of processes both the twist-three collinear formalism and a full gauge-invariant TMD approach have been developed and factorization has been proven [28–31]. Moreover, it has been shown that when the value of the small observed scale is intermediate between the typical QCD nonperturbative scale and the large factorization scale, the two approaches are mutually consistent [32–34].

In the TMD approach to DY (SIDIS) processes color gauge invariance is ensured by the inclusion of gauge links (Wilson lines), accounting for initial (final) state interactions among the struck partons involved in the hard process and the remnants of the parent hadrons (additional final state interactions are also present in the fragmentation process). Single-spin and azimuthal asymmetries are generated by TMD polarized partonic distribution and fragmentation functions, among which the most relevant from a phenomenological point of view are the Sivers distribution [35,36] and, for transversely polarized quarks, the Boer-Mulders distribution [37] and the Collins fragmentation function [38] (similar functions can be defined for linearly polarized gluons; see, e.g., Ref. [39]).

For inclusive forward pion production the large transverse single-spin asymmetry observed can be generated both by the Sivers and the Collins effects; unfortunately, these contributions cannot be disentangled and one has to consider alternative measurements in order to separate the different mechanisms. This is at variance with the case of SIDIS and DY processes, where the Sivers and Collins effects (and several other possible contributions to the azimuthal asymmetries) can be disentangled. In hadronic collisions one has to resort to different processes, e.g., the DY process (no fragmentation), single photon or jet production, two-particle (jet) production with transverse momentum imbalance, and so on.

From this point of view, a very interesting process is $pp \to \text{jet} + \pi + X$, where one observes a large p_T jet and looks for the azimuthal distribution of leading pions inside the jet. In this case, one should observe a symmetric pion distribution for the fragmentation of an unpolarized parton jet, and a $\cos\phi$ ($\cos 2\phi$) distribution for a transversely (linearly) polarized quark (gluon) parton jet (ϕ indicates the azimuthal angle of the leading pion distribution around the jet axis). Therefore, despite the complexity of the measurement (which is, however, at reach and presently under active investigation at RHIC), this process might offer plenty of new information as compared to single inclusive pion production. It would in principle allow us to disentangle the contributions coming from the Sivers and the Collins effects. Other contributions involving different combinations of TMD distribution and fragmentation functions could also be disentangled. Finally, it could also help in identifying jets coming from quark or gluon fragmentation, since the pion azimuthal distribution is different in the two cases. At RHIC kinematics a careful tuning of the kinematical configuration considered can help from this point of view.

Motivated by these considerations, in this paper we will present, in the approach of the TMD generalized parton model, and allowing for intrinsic parton motion both in the initial colliding hadrons and in the fragmentation process (which is crucial), the general expression for the polarized cross section for the process $p^\uparrow p \to \text{jet} + \pi + X$, and the structure of the azimuthal asymmetries that can be measured in the distribution of leading pions around the jet thrust axis (coinciding in our scheme with the final scattered-parton direction of motion). A very preliminary version of this study was first presented in Ref. [40]. A similar analysis was discussed in Ref. [41], which, however, considered intrinsic parton motion only in the fragmentation process, drastically reducing the possible contributions to the asymmetry. Indeed, in that case, only the Collins effect for quarks is at work. In fact, Ref. [41] aimed at studying only the Collins fragmentation function (FF), which should be universal, in a more simplified theoretical scheme for which factorization has been proven. Our approach is different in some respects. It is more general and has in principle a richer structure in the observable azimuthal asymmetries, since intrinsic motion is also taken into account in the initial hadrons. However, since factorization has not been proven in this case, but is rather taken as a reasonable phenomenological assumption, the validity of the scheme and the universality of the TMD distributions involved require an even more severe scrutiny by comparison with experimental results. On the other hand, at the present theoretical and experimental stage, we believe that combined phenomenological tests of different approaches are required to clarify the validity of factorization and, related to this, the relevance of possible universality-breaking terms for the TMD distributions.

The plan of the paper is the following. In Sec. II we will summarize the TMD generalized parton model approach,

which has been presented and discussed at length in a series of papers (see, e.g., Refs. [39,42,43]). We will then present the expression of the polarized cross section for the process of interest, discussing in detail the different partonic contributions to the process; we will finally list the azimuthal asymmetries that can be measured and their physical content. In Sec. III we will present phenomenological results for the azimuthal asymmetries discussed in the kinematical configuration of the RHIC experiments, at different c.m. energies and for central- and forward-rapidity jet production. In particular, we will first present results for the totally maximized effects, by taking all TMD functions saturated to natural positivity bounds and adding in sign all possible partonic contributions. This will assess the potential phenomenological relevance of each effect. We will then consider more carefully those effects involving the Sivers and Boer-Mulders distributions and the Collins fragmentation function, for which phenomenological parametrizations obtained by fitting combined data for azimuthal asymmetries in SIDIS, Drell-Yan, and e^+e^- collisions are available. Section IV contains our final remarks and conclusions.

II. FORMALISM

In this section we present and summarize the expressions of the polarized cross section and of the measurable azimuthal asymmetries for the process $A^{\uparrow}B \to \text{jet} + \pi + X$, where A and B are typically a pp or $p\bar{p}$ pair. Since most of the formalism has been already presented in Refs. [39,42,43], we will shortly recall the main ingredients of the approach, discussing more extensively only relevant details specific to the process considered.

Within a generalized TMD parton model approach including spin and intrinsic parton motion effects, and assuming factorization, the invariant differential cross section for the process $A(S_A)B \to \text{jet} + \pi + X$ can be written, at leading twist in the soft TMD functions, as follows:

$$\frac{E_j d\sigma^{A(S_A)B\to\text{jet}+\pi+X}}{d^3\boldsymbol{p}_j dz d^2\boldsymbol{k}_{\perp\pi}} = \sum_{a,b,c,d,\{\lambda\}} \int \frac{dx_a dx_b}{16\pi^2 x_a x_b s} d^2\boldsymbol{k}_{\perp a} \times d^2\boldsymbol{k}_{\perp b} \rho^{a/A,S_A}_{\lambda_a\lambda'_a} \hat{f}_{a/A,S_A}(x_a,\boldsymbol{k}_{\perp a}) \rho^{b/B}_{\lambda_b\lambda'_b} \hat{f}_{b/B}(x_b,\boldsymbol{k}_{\perp b}) \times \hat{M}_{\lambda_c,\lambda_d;\lambda_a,\lambda_b} \hat{M}^*_{\lambda'_c,\lambda_d;\lambda'_a,\lambda'_b} \delta(\hat{s}+\hat{t}+\hat{u}) \hat{D}^{\pi}_{\lambda_c,\lambda'_c}(z,\boldsymbol{k}_{\perp\pi}). \quad (1)$$

In an LO pQCD approach the scattered parton c in the hard elementary process $ab \to cd$ is identified with the observed fragmentation jet. Let us summarize briefly the physical meaning of the terms in Eq. (1). Full details and technical aspects can be found in Refs. [39,42,43].

We sum over all allowed partonic processes contributing to the physical process observed. $\{\lambda\}$ stays for a sum over all partonic helicities, $\lambda = \pm 1/2 (\pm 1)$ for quark (gluon) partons, respectively. $x_{a,b}$ and $\boldsymbol{k}_{\perp a,b}$ are, respectively, the initial parton light-cone momentum fractions and intrinsic transverse momenta. Analogously, z and $\boldsymbol{k}_{\perp\pi}$ are the light-cone momentum fraction and the transverse momentum of the observed pion inside the jet with respect to (w.r.t.) the jet (parton c) direction of motion.

$\rho^{a/A,S_A}_{\lambda_a\lambda'_a} \hat{f}_{a/A,S_A}(x_a,\boldsymbol{k}_{\perp a})$ contains all information on the polarization state of the initial parton a, which depends in turn on the (experimentally fixed) parent hadron A polarization state and on the soft, nonperturbative dynamics encoded in the eight leading-twist polarized and transverse momentum–dependent parton distribution functions, which will be discussed in the following. $\rho^{a/A,S_A}_{\lambda_a\lambda'_a}$ is the helicity density matrix of parton a. Analogously, the polarization state of parton b inside the unpolarized hadron B is encoded into $\rho^{b/B}_{\lambda_b\lambda'_b} \hat{f}_{b/B}(x_b,\boldsymbol{k}_{\perp b})$.

The $\hat{M}_{\lambda_c,\lambda_d;\lambda_a,\lambda_b}$'s are the pQCD leading-order helicity scattering amplitudes for the hard partonic process $ab \to cd$.

The $\hat{D}^{\pi}_{\lambda_c,\lambda'_c}(z,\boldsymbol{k}_{\perp\pi})$'s are the soft leading-twist TMD fragmentation functions describing the fragmentation process of the scattered (polarized) parton c into the final leading pion inside the jet.

As already said, we will consider as initial particles A, B, two spin-1/2 hadrons (typically, two protons) with hadron B unpolarized and hadron A in a pure transverse spin state denoted by S_A, with polarization (pseudo)vector $\boldsymbol{P}^A$.

E_j and $\boldsymbol{p}_j$ are, respectively, the energy and three-momentum of the observed jet.

Unless otherwise stated, we will always work in the AB hadronic c.m. frame, with hadron A moving along the $+\hat{\boldsymbol{Z}}_{\text{cm}}$ direction; we will define $(XZ)_{\text{cm}}$ as the production plane containing the colliding beams and the observed jet, with $(\boldsymbol{p}_j)_{X_{\text{cm}}} > 0$. We therefore have, neglecting all masses (see also Fig. 1):

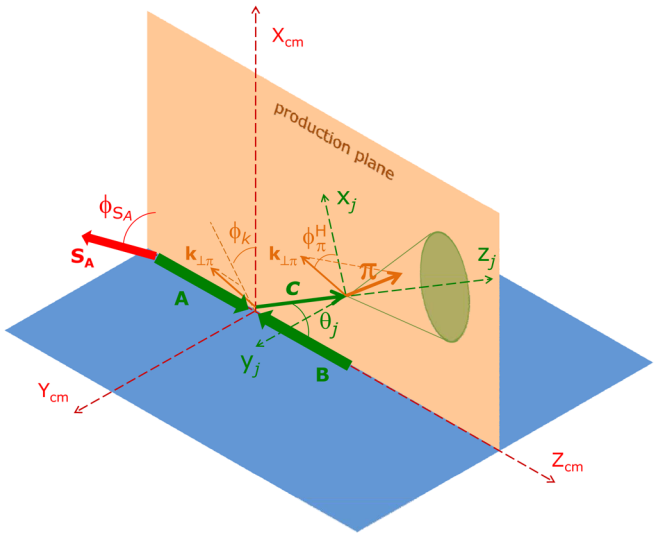

FIG. 1 (color online). Kinematical configuration for the process $A(S_A)B \to \text{jet} + \pi + X$ in the hadronic c.m. reference frame.

$$
\begin{aligned}
p_A^\mu &= \frac{\sqrt{s}}{2}(1,0,0,1)\\
S_A^\mu &= S_T^\mu = (0,\cos\phi_{S_A},\sin\phi_{S_A},0)\\
p_B^\mu &= \frac{\sqrt{s}}{2}(1,0,0,-1)\\
p_a^\mu &= \left(x_a\frac{\sqrt{s}}{2}+\frac{\boldsymbol{k}_{\perp a}^2}{2x_a\sqrt{s}}, k_{\perp a}\cos\phi_a, k_{\perp a}\sin\phi_a,\right.\\
&\qquad \left. x_a\frac{\sqrt{s}}{2}-\frac{\boldsymbol{k}_{\perp a}^2}{2x_a\sqrt{s}}\right)\\
p_b^\mu &= \left(x_b\frac{\sqrt{s}}{2}+\frac{\boldsymbol{k}_{\perp b}^2}{2x_b\sqrt{s}}, k_{\perp b}\cos\phi_b, k_{\perp b}\sin\phi_b,\right.\\
&\qquad \left. -x_b\frac{\sqrt{s}}{2}+\frac{\boldsymbol{k}_{\perp b}^2}{2x_b\sqrt{s}}\right)\\
p_c^\mu &\equiv p_{\rm j}^\mu = (E_{\rm j}, p_{{\rm j}T}, 0, p_{{\rm j}L}) = E_{\rm j}(1,\sin\theta_{\rm j},0,\cos\theta_{\rm j})\\
&= p_{{\rm j}T}(\cosh\eta_{\rm j},1,0,\sinh\eta_{\rm j})\\
p_\pi^\mu &= E_\pi(1,\sin\theta_\pi\cos\phi_\pi,\sin\theta_\pi\sin\phi_\pi,\cos\theta_\pi),
\end{aligned}
\tag{2}
$$

where $\eta_{\rm j}$ is the jet (pseudo)rapidity, $\eta_{\rm j} = -\log[\tan(\theta_{\rm j}/2)]$.

Notice that, since the observed jet is identified with the scattered parton c, the helicity frame of the fragmenting parton, whose z axis, $\hat{\boldsymbol{z}}_{\rm j}$, is along the direction of motion of parton c, is related to the hadronic c.m. frame by a simple rotation by $\theta_{\rm j}$ around $\hat{\boldsymbol{Y}}_{\rm cm} \equiv \hat{\boldsymbol{y}}_{\rm j}$. In this frame ($\hat{\boldsymbol{z}}_{\rm j}$ identifies also the jet light-cone direction) we have:

$$
\begin{aligned}
\tilde{p}_c^\mu &= \tilde{p}_{\rm j}^\mu = E_{\rm j}(1,0,0,1)\\
\tilde{p}_\pi^\mu &= \left(E_\pi, \boldsymbol{k}_{\perp\pi}, \sqrt{E_\pi^2-\boldsymbol{k}_{\perp\pi}^2}\right)\\
&= \left(E_\pi, k_{\perp\pi}\cos\phi_\pi^H, k_{\perp\pi}\sin\phi_\pi^H, \sqrt{E_\pi^2-\boldsymbol{k}_{\perp\pi}^2}\right),
\end{aligned}
\tag{3}
$$

where ϕ_π^H is the azimuthal angle of the pion three-momentum around the jet direction of motion, as measured in the fragmenting parton helicity frame.

The light-cone momentum fraction of the observed pion is given by

$$
z = \frac{p_\pi^+}{p_c^+} \equiv \frac{p_\pi^+}{p_{\rm j}^+} = \frac{E_\pi + \sqrt{E_\pi^2-\boldsymbol{k}_{\perp\pi}^2}}{2E_{\rm j}}. \tag{4}
$$

We can also write, respectively, in the jet (parton c) helicity frame and in the hadronic c.m. frame:

$$
\begin{aligned}
\boldsymbol{p}_\pi &= k_{\perp\pi}\cos\phi_\pi^H\hat{\boldsymbol{x}}_{\rm j} + k_{\perp\pi}\sin\phi_\pi^H\hat{\boldsymbol{y}}_{\rm j} + \sqrt{E_\pi^2-\boldsymbol{k}_{\perp\pi}^2}\,\hat{\boldsymbol{z}}_{\rm j}\\
&= \left[k_{\perp\pi}\cos\phi_\pi^H\cos\theta_{\rm j} + \sqrt{E_\pi^2-\boldsymbol{k}_{\perp\pi}^2}\sin\theta_{\rm j}\right]\hat{\boldsymbol{X}}_{\rm cm}\\
&\quad + k_{\perp\pi}\sin\phi_\pi^H\hat{\boldsymbol{Y}}_{\rm cm} + \left[-k_{\perp\pi}\cos\phi_\pi^H\sin\theta_{\rm j}\right.\\
&\quad \left. + \sqrt{E_\pi^2-\boldsymbol{k}_{\perp\pi}^2}\cos\theta_{\rm j}\right]\hat{\boldsymbol{Z}}_{\rm cm}.
\end{aligned}
\tag{5}
$$

Let us stress that in our notation intrinsic transverse momenta, $\boldsymbol{k}_{\perp i}$, $i = a, b, \pi$, are always 3-vectors and $k_{\perp i} \equiv |\boldsymbol{k}_{\perp i}|$. This has to be kept in mind when comparing with literature, where often intrinsic momenta are intended as 4-vectors and $k_\perp^2 = -\boldsymbol{k}_\perp^2$. From Eq. (5) it is easy to see that the pion intrinsic transverse momentum is given, in the hadronic c.m. frame, by

$$
\begin{aligned}
\boldsymbol{k}_{\perp\pi} &= k_{\perp\pi}\cos\phi_\pi^H\cos\theta_{\rm j}\hat{\boldsymbol{X}}_{\rm cm} + k_{\perp\pi}\sin\phi_\pi^H\hat{\boldsymbol{Y}}_{\rm cm}\\
&\quad - k_{\perp\pi}\cos\phi_\pi^H\sin\theta_{\rm j}\hat{\boldsymbol{Z}}_{\rm cm}.
\end{aligned}
\tag{6}
$$

Defining by ϕ_k the azimuthal angle of the pion intrinsic transverse momentum, $\boldsymbol{k}_{\perp\pi}$, *as measured in the hadronic c.m. frame* (see Fig. 1), from Eq. (6) we easily see that

$$
\tan\phi_k = \frac{\tan\phi_\pi^H}{\cos\theta_{\rm j}}. \tag{7}
$$

Notice that, for central rapidity jets ($\theta_{\rm j} = \pi/2$), $\phi_k = \pi/2$. Therefore, azimuthal asymmetries modulated in terms of ϕ_k are artificially suppressed in the central rapidity region, while the physically relevant angle is ϕ_π^H. Instead, in the forward rapidity region, when $\cos\theta_{\rm j} \to 1$, the two angles are practically coincident. Notice also that in Ref. [41], where only the forward rapidity region was considered, the angle ϕ_k (called ϕ_h there) was adopted.

Let us now come back to the soft TMD partonic distribution and fragmentation functions entering the differential cross section for the process $A(S_A)B \to \text{jet} + \pi + X$, Eq. (1). Consider first the polarized soft process at the distribution level, $A(S_A) \to a + X$; as said, in Eq. (1) all information on this process is encoded in the factor $\rho^{a/A,S_A}_{\lambda_a\lambda_a'}\hat{f}_{a/A,S_A}(x_a,\boldsymbol{k}_{\perp a})$. This factor depends on the polarization state (fixed by experimental conditions) of the parent hadron A, described by its own helicity density matrix ρ^{A,S_A}, and on generalized soft distribution functions for the process $A(S_A) \to a + X$, $\hat{F}^{\lambda_a,\lambda_a'}_{\lambda_A,\lambda_A'}(x_a,\boldsymbol{k}_{\perp a})$:

$$
\rho^{a/A,S_A}_{\lambda_a\lambda_a'}\hat{f}_{a/A,S_A}(x_a,\boldsymbol{k}_{\perp a}) = \sum_{\lambda_A,\lambda_A'}\rho^{A,S_A}_{\lambda_A,\lambda_A'}\hat{F}^{\lambda_a,\lambda_a'}_{\lambda_A,\lambda_A'}(x_a,\boldsymbol{k}_{\perp a}). \tag{8}
$$

The functions $\hat{F}^{\lambda_a,\lambda_a'}_{\lambda_A,\lambda_A'}$ are related to the well-known leading-twist handbag diagram for deeply inelastic scattering. Analogous relations hold for parton b inside the (un)polarized hadron B.

Rotational invariance and parity conservation for strong interactions imply some very general relations for these nonperturbative functions:

$$
\hat{F}^{\lambda_a,\lambda_a'}_{\lambda_A,\lambda_A'}(x_a,\boldsymbol{k}_{\perp a}) = F^{\lambda_a,\lambda_a'}_{\lambda_A,\lambda_A'}(x_a,k_{\perp a})e^{i(\lambda_A-\lambda_A')\phi_a}, \tag{9}
$$

where ϕ_a is the azimuthal angle of parton a intrinsic transverse momentum, $\boldsymbol{k}_{\perp a}$, in the parent hadron A helicity frame (coinciding in the present case with the hadronic c.m. frame). Notice that the *reduced* soft functions F on the right-hand side (without the hat) do not depend anymore on azimuthal phases. Moreover,

$$F^{-\lambda_a,-\lambda'_a}_{-\lambda_A,-\lambda'_A}(x_a,k_{\perp a}) = (-1)^{(S_A-s_a)} \times (-1)^{(\lambda_A-\lambda_a)+(\lambda'_A-\lambda'_a)} F^{\lambda_a,\lambda'_a}_{\lambda_A,\lambda'_A}(x_a,k_{\perp a}), \tag{10}$$

where S_A and s_a are the spins of the parent hadron and of the parton, respectively. Notice that for spin-1/2 colliding hadrons, $S_A = 1/2$, the factor $(-1)^{(S_A-s_a)}$ is positive (negative) for quark (gluon) partons, and therefore some parity properties of the soft functions are different for quarks and gluons. By combining complex conjugation and parity properties, one can show that some of these functions are purely real or purely imaginary. As a result, for spin-1/2 hadrons only eight independent soft distributions survive at leading twist. They can be easily related to the TMD distributions widely discussed in the literature. Before listing them for completeness, let us recall another important property of the hadronic functions $F^{\lambda_a\lambda'_a}_{\lambda_A\lambda'_A}(x_a,k_{\perp a})$, coming from total angular momentum conservation in the forward direction, that is, for $k_{\perp a} \to 0$:

$$F^{\lambda_a,\lambda'_a}_{\lambda_A,\lambda'_A}(x_a,k_{\perp a}) \sim \left(\frac{k_{\perp a}}{M}\right)^{|\lambda_A-\lambda_a-(\lambda'_A-\lambda'_a)|} \tilde{F}^{\lambda_a,\lambda'_a}_{\lambda_A,\lambda'_A}(x_a,k_{\perp a}), \tag{11}$$

where M is a typical hadronic mass scale and the $\tilde{F}$'s stay for the remaining part of the functions that, depending on the details of dynamics, may or may not vanish in the collinear configuration. The relevant hadronic functions and their connection with the leading-twist TMD distributions is therefore, in the quark case (for clarity we adopt here both the notation of Ref. [39] and that of the Amsterdam group [22,37,44]),

$$\begin{aligned}
F^{++}_{q++}(x,k_\perp) + F^{--}_{q++}(x,k_\perp) &= f_{q/A}(x,k_\perp) = f_1^q(x,k_\perp)\\
F^{++}_{q++}(x,k_\perp) - F^{--}_{q++}(x,k_\perp) &= \Delta_L f_{q/A}(x,k_\perp) = g^q_{1L}(x,k_\perp)\\
F^{+-}_{q+-}(x,k_\perp) &= h_1^q(x,k_\perp)\\
F^{-+}_{q+-}(x,k_\perp) &= \frac{k_\perp^2}{2M^2} h^{\perp q}_{1T}(x,k_\perp)\\
\mathrm{Re}F^{++}_{q+-}(x,k_\perp) &= \frac{k_\perp}{2M} g^{\perp q}_{1T}(x,k_\perp)\\
\mathrm{Im}F^{++}_{q+-}(x,k_\perp) &= \frac{1}{4}\Delta^N f_{q/A^\uparrow}(x,k_\perp)\\
&= -\frac{k_\perp}{2M} f^{\perp q}_{1T}(x,k_\perp)\\
\mathrm{Re}F^{+-}_{q++}(x,k_\perp) &= \frac{k_\perp}{2M} h^{\perp q}_{1L}(x,k_\perp)\\
\mathrm{Im}F^{+-}_{q++}(x,k_\perp) &= -\frac{1}{2}\Delta^N f_{q^\uparrow/A}(x,k_\perp)\\
&= \frac{k_\perp}{2M} h_1^{\perp q}(x,k_\perp).
\end{aligned} \tag{12}$$

Analogous relations hold for gluon partons with the changes discussed above, due to the different spin of the parton and leading to different parity properties. Notice that instead of transversely polarized quarks we will have linearly polarized gluons. Of course, the same relations hold also for the $B \to b + X$ process. However, this time the $\hat{\boldsymbol{X}}_B$ and $\hat{\boldsymbol{Z}}_B$ axes of hadron B helicity frame are opposite to those of the hadronic c.m. frame.

Concerning the fragmentation process, since here we are considering only pions (in general, unpolarized hadrons), the discussion of the soft fragmentation functions, $\hat{D}^{\pi}_{\lambda_c,\lambda'_c}$, is much simplified. In practice, only two independent TMD fragmentation functions survive: one with diagonal parton helicity indexes, related to the TMD unpolarized FF,

$$\hat{D}^{\pi/c}_{\pm\pm}(z,\boldsymbol{k}_{\perp\pi}) \equiv D^{\pi/c}_{\pm\pm}(z,k_{\perp\pi}) = D_{\pi/c}(z,k_{\perp\pi}), \tag{13}$$

and a second one with off-diagonal parton helicity indexes, $\hat{D}^{\pi/c}_{+-}(z,\boldsymbol{k}_{\perp\pi})$. This second function is purely imaginary for quark partons and is related to the well-known Collins function [38], describing the fragmentation of a transversely polarized quark into a noncollinear unpolarized hadron. Instead, for gluon partons the analogous Collins-like function is purely real and is related to the fragmentation of linearly polarized gluons again into an unpolarized hadron.

It is very important to realize that these off-diagonal quark and gluon TMD FFs have different behaviors as a function of the azimuthal angle of the observed pion around the direction of motion of the fragmentation jet. More specifically, for quarks we have

$$\hat{D}^{\pi/q}_{\pm\mp}(z,\boldsymbol{k}_{\perp\pi}) = \pm D^{\pi/q}_{+-}(z,k_{\perp\pi}) e^{\pm i\phi^H_\pi}, \tag{14}$$

while for gluons the analogous relation reads

$$\hat{D}^{\pi/g}_{\pm\mp}(z,\boldsymbol{k}_{\perp\pi}) = D^{\pi/g}_{+-}(z,k_{\perp\pi}) e^{\pm i2\phi^H_\pi}. \tag{15}$$

As mentioned above, the azimuthal independent parts of these TMD FFs are related to the probability for a transversely (linearly) polarized quark (gluon) of fragmenting into a noncollinear unpolarized hadron, the Collins (Collins-like for gluons) fragmentation function [39],

$$\begin{aligned}
D^{\pi/q}_{+-}(z,k_{\perp\pi}) &= \frac{i}{2}\Delta^N D_{\pi/q^\uparrow}(z,k_{\perp\pi}) = \frac{i}{2}\frac{k_{\perp\pi}}{zm_\pi} H_1^\perp(z,k_{\perp\pi})\\
D^{\pi/g}_{+-}(z,k_{\perp\pi}) &= \frac{1}{2}\Delta^N D_{\pi/\mathcal{T}^g_1}(z,k_{\perp\pi}).
\end{aligned} \tag{16}$$

Again, total angular momentum conservation in the forward direction dictates the power behavior of the TMD FFs for $k_{\perp\pi} \to 0$:

$$D^{\pi}_{\lambda_c,\lambda_c'}(z,k_{\perp\pi}) \sim \left(\frac{k_{\perp\pi}}{M}\right)^{|\lambda_c-\lambda_c'|} \tilde{D}^{\pi}_{\lambda_c,\lambda_c'}(z,k_{\perp\pi}). \tag{17}$$

In this case as well, the behavior of the off-diagonal FFs is different for quarks and gluons.

Let us finally comment on the helicity amplitudes for the partonic hard-scattering processes entering Eq. (1). Again, details have already been presented in Refs. [39,43], and here we limit ourselves to summarizing some useful properties. Because of intrinsic partonic motion in the distributions and in the fragmentation process, the general kinematical configuration for the partonic process $ab \to cd$ is not planar in the hadronic c.m. frame. Since partons can in general be polarized in the process, azimuthal phases are therefore essential and must be properly taken into account. For massless partons, due to helicity conservation in the quark-gluon vertex and parity invariance only three independent helicity amplitudes survive:

$$\begin{aligned}
\hat{M}_{++;++} &= \hat{M}^*_{--;--} = \hat{M}^0_1 e^{i\varphi_1} \\
\hat{M}_{-+;-+} &= \hat{M}^*_{+-;+-} = \hat{M}^0_2 e^{i\varphi_2} \\
\hat{M}_{-+;+-} &= \hat{M}^*_{+-;-+} = \hat{M}^0_3 e^{i\varphi_3}.
\end{aligned} \tag{18}$$

Here $\pm$ stays for $\lambda = \pm 1/2$ for quarks and $\lambda = \pm 1$ for gluons. $\hat{M}^0_i$ $(i = 1, 2, 3)$ are the three independent helicity amplitudes in the canonical partonic c.m. frame, that is, a frame where partons a, b move along the $\pm\hat{z}$ direction, respectively, and the scattering plane coincides with the (xz) plane. The phases φ_i collect all azimuthal phases coming from rotations and boosts connecting the canonical partonic c.m. frame with the hadronic c.m. frame adopted in the paper. Their general expression is rather involved. All details and the explicit expressions of the $\hat{M}^0_i$ and φ_i can be found in Refs. [39,43]. Here we limit ourselves to noting that for parton c lying in the $(XZ)_{\rm cm}$ plane, as in the present case, the phases φ_i are odd under $\boldsymbol{k}_{\perp a,b} \to -\boldsymbol{k}_{\perp a,b}$. This property, as we will see below, is very helpful in selecting only physically observable effects out of the many contributions present in Eq. (1) because of the nonplanarity of the partonic process: in fact, some of these contributions do not survive at the hadronic level under integration over intrinsic parton momenta.

We now concentrate on the partonic kernels entering the expression of the polarized cross section, Eq. (1):

$$\begin{aligned}
\Sigma(S_A)^{ab\to cd} = &\sum_{\{\lambda\}} \rho^{a/A,S_A}_{\lambda_a\lambda_a'} \hat{f}_{a/A,S_A}(x_a,\boldsymbol{k}_{\perp a}) \\
&\times \rho^{b/B}_{\lambda_b\lambda_b'} \hat{f}_{b/B}(x_b,\boldsymbol{k}_{\perp b}) \hat{M}_{\lambda_c,\lambda_d;\lambda_a,\lambda_b} \\
&\times \hat{M}^*_{\lambda_c',\lambda_d;\lambda_a',\lambda_b'} \hat{D}^{\pi}_{\lambda_c,\lambda_c'}(z,\boldsymbol{k}_{\perp\pi}).
\end{aligned} \tag{19}$$

One has to evaluate the kernels for each of the eight distinct partonic channels contributing to the cross section,

$$\begin{aligned}
&qq \to qq, \quad qg \to qg, \quad qg \to gq, \quad gq \to qg, \\
&gq \to gq \quad gg \to q\bar{q}, \quad q\bar{q} \to gg, \quad gg \to gg,
\end{aligned} \tag{20}$$

where in the first line q stays for both quarks and antiquarks in all allowed combinations.

In practice, the calculation is performed by summing explicitly over all helicity indexes and inserting the appropriate expressions for the helicity density matrices of partons a, b and for the polarized distribution and fragmentation functions, as detailed above. Furthermore, after factorizing explicitly all azimuthal dependencies, including those coming from the hard-scattering helicity amplitudes, collecting them and using symmetry properties under $\boldsymbol{k}_{\perp a,b} \to -\boldsymbol{k}_{\perp a,b}$, one gets the final expression for the kernels, containing only physically allowed terms at the hadronic level.

We will not present explicitly the kernels for all channels. Instead, we limit ourselves to giving the kernels for the $qq \to qq$ and $gg \to gg$ channels, which contain the maximal number of terms and give examples of possible contributions involving both quark and gluon distribution and fragmentation functions. Moreover, we will directly present the combination of kernels, $\Sigma(\phi_{S_A}) \pm \Sigma(\phi_{S_A} + \pi)$, entering the numerator and the denominator of the single-spin azimuthal asymmetries discussed in the sequel. We will also omit for shortness the explicit dependencies on the light-cone momentum fractions and intrinsic momenta of all TMD distribution and fragmentation functions. On the contrary, all azimuthal dependencies are explicitly shown. In particular, terms are collected according to the azimuthal dependencies in the fragmentation process which directly enter the azimuthal asymmetries we want to study. Therefore, we get for the $qq \to qq$ channel:

$$\begin{aligned}
[\Sigma(\phi_{S_A}) + \Sigma(\phi_{S_A} + \pi)]^{qq\to qq} \sim &\{f_{a/A} f_{b/B} [|\hat{M}^0_1|^2 \\
&+ |\hat{M}^0_2|^2 + |\hat{M}^0_3|^2] - 2\Delta^N f_{a^\uparrow/A} \Delta^N f_{b^\uparrow/B} \hat{M}^0_2 \hat{M}^0_3 \\
&\times \cos(\varphi_2 - \varphi_3)\} D_{\pi/q} + \{\Delta^N f_{a^\uparrow/A} f_{b/B} \hat{M}^0_1 \hat{M}^0_2 \\
&\times \cos(\varphi_1 - \varphi_2) - f_{a/A} \Delta^N f_{b^\uparrow/B} \hat{M}^0_1 \hat{M}^0_3 \cos(\varphi_1 - \varphi_3)\} \\
&\times \Delta^N D_{\pi/q^\uparrow} \cos\phi^H_\pi.
\end{aligned} \tag{21}$$

The symbol $\sim$ is to recall that, as discussed above, this expression is valid only after integrating over the azimuthal angles of the initial intrinsic parton momenta, $\boldsymbol{k}_{\perp a,b}$, and is based on symmetry properties of the kernels under $\boldsymbol{k}_{\perp a,b} \to -\boldsymbol{k}_{\perp a,b}$. It contains fewer terms than the general expression for the kernels in the $\boldsymbol{k}_{\perp a,b}$-unintegrated, nonplanar partonic configuration.

Analogously, for the numerator of the asymmetry, we find:

$$
\begin{aligned}
[\Sigma(\phi_{S_A}) - \Sigma(\phi_{S_A} + \pi)]^{qq\to qq} \sim & \left\{ \frac{1}{2}\Delta^N f_{a/A^\uparrow} f_{b/B} \cos\phi_a [|\hat{M}_1^0|^2 + |\hat{M}_2^0|^2 + |\hat{M}_3^0|^2] \right. \\
& \left. - h_1^q \Delta^N f_{b^\uparrow/B} \cos(\phi_a - \varphi_2 + \varphi_3) 2\hat{M}_2^0 \hat{M}_3^0 + \frac{k_{\perp a}^2}{2M^2} h_{1T}^{\perp a} \Delta^N f_{b^\uparrow/B} \cos(\phi_a + \varphi_2 - \varphi_3) 2\hat{M}_2^0 \hat{M}_3^0 \right\} \sin\phi_{S_A} D_{\pi/q} \\
& + \left\{ -\frac{1}{2}\Delta^N f_{a/A^\uparrow} \Delta^N f_{b^\uparrow/B} \cos\phi_a \cos(\varphi_1 - \varphi_3) \hat{M}_1^0 \hat{M}_3^0 + h_1^a f_{b/B} \cos(\phi_a + \varphi_1 - \varphi_2) \hat{M}_1^0 \hat{M}_2^0 \right. \\
& \left. - \frac{k_{\perp a}^2}{2M^2} h_{1T}^{\perp a} f_{b/B} \cos(\phi_a - \varphi_1 + \varphi_2) \hat{M}_1^0 \hat{M}_2^0 \right\} \sin\phi_{S_A} \Delta^N D_{\pi/q^\uparrow} \cos\phi_\pi^H \\
& + \left\{ -\frac{1}{2}\Delta^N f_{a/A^\uparrow} \Delta^N f_{b^\uparrow/B} \sin\phi_a \sin(\varphi_1 - \varphi_3) \hat{M}_1^0 \hat{M}_3^0 - h_1^a f_{b/B} \cos(\phi_a + \varphi_1 - \varphi_2) \hat{M}_1^0 \hat{M}_2^0 \right. \\
& \left. - \frac{k_{\perp a}^2}{2M^2} h_{1T}^{\perp a} f_{b/B} \cos(\phi_a - \varphi_1 + \varphi_2) \hat{M}_1^0 \hat{M}_2^0 \right\} \cos\phi_{S_A} \Delta^N D_{\pi/q^\uparrow} \sin\phi_\pi^H . \qquad (22)
\end{aligned}
$$

Let us discuss the physical content of these results. Equation (21) gives the contribution of the $qq \to qq$ channel to (twice) the unpolarized cross section. It contains two terms azimuthally symmetric in the fragmentation process: the first is the usual term already present in the collinear factorization scheme, the second one is the possible contribution due to the Boer-Mulders effect coming from both initial partons.

The last two terms in Eq. (21) might potentially give rise to an azimuthal asymmetry in the jet $\to \pi + X$ *unpolarized* process: they are related to the combined action of the Boer-Mulders function (either for parton quark a or b, separately) and of the Collins fragmentation function. Notice that only the first contribution in Eq. (21) survives in a purely collinear scheme, or even in a scheme like that adopted in Refs. [41,45,46], where intrinsic motion is kept into account only in the fragmentation process.

Equation (22) is related to transverse spin asymmetries for pion production inside a jet. Again, it contains terms related to the unpolarized pion fragmentation function $D_{\pi/q}(z, k_{\perp\pi})$ which are symmetric with respect to ϕ_π^H, and terms proportional to the Collins fragmentation function which are responsible for the azimuthal asymmetries in the jet fragmentation process.

The first group of terms, proportional to $D_{\pi/q}$, are related to a single-spin asymmetry (only hadron A is polarized). The only contribution allowed by rotational invariance and parity conservation comes from hadron A being polarized transversely to the jet production plane, which explains the $\sin\phi_{S_A}$ factor.

Notice once more that the appearance of only the physically allowed contributions is not trivial in our expression, which, at this stage, is still unintegrated over $\boldsymbol{k}_{\perp a,b}$. However, as discussed above, taking into account symmetry properties under $\boldsymbol{k}_{\perp a,b} \to -\boldsymbol{k}_{\perp a,b}$ amounts to select from the beginning only physically allowed contributions from the wealth of partonic terms present in the general nonplanar configuration for the partonic process.

In the case of Eq. (22) the terms proportional to $D_{\pi/q}$ come from the Sivers effect (first term) and from combinations of the transversity and the Boer-Mulders functions for partons a and b, respectively.

Let us now consider the terms in Eq. (22) related to the Collins fragmentation function, $\Delta^N D_{\pi/q^\uparrow}$. These refer effectively to a double-spin asymmetry, since both hadron A and the final quark c (generating the observed jet) are transversely polarized. Their physical content is also easy to understand. The first three terms, proportional to $\Delta^N D_{\pi/q^\uparrow} \sin\phi_{S_A}$, correspond to a double transverse spin asymmetry, where both hadron A and the final parton c are transversely polarized w.r.t. the jet production plane, along the $\hat{\boldsymbol{Y}}_{\rm cm}$ axis. In this case, the Collins effect in the fragmentation process survives only for the component of the pion transverse momentum (w.r.t. the jet) orthogonal to the parton c polarization vector, that is, the component lying in the production plane, which explains the associated $\cos\phi_\pi^H$ factor (see Fig. 1).

Analogously, the three terms proportional to $\Delta^N D_{\pi/q^\uparrow} \cos\phi_{S_A}$ correspond again to a double transverse spin asymmetry, this time for hadron A and the final parton c transversely polarized w.r.t. their own direction of motion but in the production plane (i.e., along the x axis of the respective helicity frames). Again, only the component of the pion transverse momentum orthogonal to the parton c polarization vector contributes to the Collins asymmetry in the fragmentation process, which is this time guaranteed by the $\sin\phi_\pi^H$ factor.

Although Eq. (22) makes the physical content of the asymmetry more evident, the following equivalent expression, where the terms proportional to the Collins FF are collected differently, makes the possible azimuthal asymmetries in the jet fragmentation process more readable:

$$[\Sigma(\phi_{S_A}) - \Sigma(\phi_{S_A}+\pi)]^{qq\to qq} \sim \Big\{\frac{1}{2}\Delta^N f_{a/A^\uparrow} f_{b/B}\cos\phi_a[|\hat{M}_1^0|^2 + |\hat{M}_2^0|^2 + |\hat{M}_3^0|^2]$$
$$- h_1^a \Delta^N f_{b^\uparrow/B}\cos(\phi_a - \varphi_2 + \varphi_3) 2\hat{M}_2^0\hat{M}_3^0 + \frac{k_{\perp a}^2}{2M^2} h_{1T}^{\perp a}\Delta^N f_{b^\uparrow/B}\cos(\phi_a + \varphi_2 - \varphi_3) 2\hat{M}_2^0\hat{M}_3^0\Big\}\sin\phi_{S_A} D_{\pi/q}$$
$$+ \Big\{[h_1^a f_{b/B}\cos(\phi_a + \varphi_1 - \varphi_2)\hat{M}_1^0\hat{M}_2^0 - \frac{1}{4}\Delta^N f_{a/A^\uparrow}\Delta^N f_{b^\uparrow/B}\cos(\phi_a + \varphi_1 - \varphi_3)\hat{M}_1^0\hat{M}_3^0]\sin(\phi_{S_A} - \phi_\pi^H)$$
$$- \Big[\frac{k_{\perp a}^2}{2M^2} h_{1T}^{\perp a} f_{b/B}\cos(\phi_a - \varphi_1 + \varphi_2)\hat{M}_1^0\hat{M}_2^0 + \frac{1}{4}\Delta^N f_{a/A^\uparrow}\Delta^N f_{b^\uparrow/B}\cos(\phi_a - \varphi_1 + \varphi_3)\hat{M}_1^0\hat{M}_3^0\Big]\sin(\phi_{S_A} + \phi_\pi^H)\Big\}$$
$$\times \Delta^N D_{\pi/q^\uparrow}. \tag{23}$$

Therefore, apart from the term proportional to $D_{\pi/q}$, two azimuthal asymmetries in the distribution of leading pions inside the jet are possible, proportional, respectively, to $\sin(\phi_{S_A} \mp \phi_\pi^H)$.

Neglecting intrinsic motion of the initial partons, $\boldsymbol{k}_{\perp a,b} \to 0$, Eqs. (21) and (23) simplify considerably:

$$[\Sigma(\phi_{S_A}) + \Sigma(\phi_{S_A}+\pi)]^{qq\to qq} \to f_{a/A}(x_a) f_{b/B}(x_b)[|\hat{M}_1^0|^2 + |\hat{M}_2^0|^2 + |\hat{M}_3^0|^2] D_{\pi/q}(z, k_{\perp\pi}), \tag{24}$$

$$[\Sigma(\phi_{S_A}) - \Sigma(\phi_{S_A}+\pi)]^{qq\to qq} \to h_1^a(x_a) f_{b/B}(x_b)\hat{M}_1^0\hat{M}_2^0\Delta^N D_{\pi/q^\uparrow}(z, k_{\perp\pi})\sin(\phi_{S_A} - \phi_\pi^H), \tag{25}$$

in agreement with the results of Ref. [41]. Notice, however, that our angle ϕ_π^H is the azimuthal angle of $\boldsymbol{k}_{\perp\pi}$ measured in the jet (parton c) helicity frame. Therefore, it does not coincide with the angle ϕ_h utilized in Ref. [41], which is the azimuthal angle of $\boldsymbol{k}_{\perp\pi}$ measured in the hadronic c.m. frame [we call this angle ϕ_k in this paper; see Eq. (7) and Fig. 1]. Only for forward jet production ($\cos\theta_j \to 1$) do these angles coincide with good approximation.

In the case of the $gg \to gg$ partonic channel, the analogues of Eqs. (21) and (23) are

$$[\Sigma(\phi_{S_A}) + \Sigma(\phi_{S_A}+\pi)]^{gg\to gg} \sim \{f_{a/A} f_{b/B}[|\hat{M}_1^0|^2 + |\hat{M}_2^0|^2 + |\hat{M}_3^0|^2] - 2\Delta^N f_{\mathcal{T}_1^a/A}\Delta^N f_{\mathcal{T}_1^b/B}\hat{M}_2^0\hat{M}_3^0\cos(\varphi_2 - \varphi_3)\} D_{\pi/g}$$
$$+ \{\Delta^N f_{\mathcal{T}_1^a/A} f_{b/B}\hat{M}_1^0\hat{M}_2^0\cos(\varphi_1 - \varphi_2) + f_{a/A}\Delta^N f_{\mathcal{T}_1^b/B}\hat{M}_1^0\hat{M}_3^0\cos(\varphi_1 - \varphi_3)\}\Delta^N D_{\pi/\mathcal{T}_1^g}\cos 2\phi_\pi^H, \tag{26}$$

$$[\Sigma(\phi_{S_A}) - \Sigma(\phi_{S_A}+\pi)]^{gg\to gg} \sim \Big\{\frac{1}{2}\Delta^N f_{a/A^\uparrow} f_{b/B}\cos\phi_a\Big[|\hat{M}_1^0|^2 + |\hat{M}_2^0|^2 + |\hat{M}_3^0|^2\Big]$$
$$+ \mathrm{Im}F_{a+-}^{+-}\Delta^N f_{\mathcal{T}_1^b/B}\cos(\phi_a - \varphi_2 + \varphi_3) 2\hat{M}_2^0\hat{M}_3^0 + \mathrm{Im}F_{a+-}^{-+}\Delta^N f_{\mathcal{T}_1^b/B}\cos(\phi_a + \varphi_2 - \varphi_3) 2\hat{M}_2^0\hat{M}_3^0\Big\}\sin\phi_{S_A} D_{\pi/g}$$
$$+ \Big\{\Big[\mathrm{Im}F_{a+-}^{+-} f_{b/B}\cos(\phi_a + \varphi_1 - \varphi_2)\hat{M}_1^0\hat{M}_2^0 + \frac{1}{4}\Delta^N f_{a/A^\uparrow}\Delta^N f_{\mathcal{T}_1^b/B}\cos(\phi_a - \varphi_1 + \varphi_3)\hat{M}_1^0\hat{M}_3^0\Big]\sin(\phi_{S_A} - 2\phi_\pi^H)$$
$$- \Big[\mathrm{Im}F_{a+-}^{-+} f_{b/B}\cos(\phi_a - \varphi_1 + \varphi_2)\hat{M}_1^0\hat{M}_2^0 + \frac{1}{4}\Delta^N f_{a/A^\uparrow}\Delta^N f_{\mathcal{T}_1^b/B}\cos(\phi_a + \varphi_1 - \varphi_3)\hat{M}_1^0\hat{M}_3^0\Big]\sin(\phi_{S_A} + 2\phi_\pi^H)\Big\}$$
$$\times \Delta^N D_{\pi/\mathcal{T}_1^g}. \tag{27}$$

The structure is the same as for the quark case, but this time all distributions related to transversely polarized quark partons and the Collins fragmentation functions are replaced by analogous functions for linearly polarized gluons; see Ref. [39] for more details. Notice that for linearly polarized gluons inside the polarized hadron A, to avoid confusion with notation we prefer to keep the definitions in terms of the functions $F_{\lambda_A,\lambda_A'}^{\lambda_a,\lambda_a'}$. It is also important to notice that this time the possible azimuthal asymmetries in the distribution of leading pions inside the (gluon) jet are proportional to $\cos 2\phi_\pi^H$ and $\sin(\phi_{S_A} \mp 2\phi_\pi^H)$, respectively, for the unpolarized and single-polarized case. Therefore, by measuring these asymmetries one should in principle be able to select contributions coming from either quark or gluon jet fragmentation.

It is easy to see that in the case of collinear initial partons Eq. (26) reduces again to the usual collinear contribution to the unpolarized cross section, while Eq. (27) vanishes. Therefore, the measurement of such types of asymmetries would be a clear indication that effects originating from intrinsic parton motion in the initial colliding hadrons are at work. From the phenomenological point of

view, this would be a crucial test for the TMD approach, independently of the open issues concerning factorization and universality of the TMD distribution functions mentioned in the introduction.

Expressions similar to those shown above for the $qq \to qq$ and $gg \to gg$ channels hold also for all partonic contributions involved, with the appropriate combinations of quark and gluon distribution and fragmentation functions. In general, fewer terms are present both in the denominator and the numerator of the asymmetry. Moreover, as a general rule distribution and fragmentation functions related to transversely (linearly) polarized quarks (gluons) appear only in couples. This limits the number of allowed terms.

According to these results, the single-transverse polarized cross section for the process $A(S_A)B \to \text{jet} + \pi + X$ will have the following general structure:

$$\begin{aligned} 2d\sigma(\phi_{S_A}, \phi_\pi^H) &\sim d\sigma_0 + d\Delta\sigma_0 \sin\phi_{S_A} + d\sigma_1 \cos\phi_\pi^H \\ &+ d\Delta\sigma_1^- \sin(\phi_{S_A} - \phi_\pi^H) + d\Delta\sigma_1^+ \sin(\phi_{S_A} + \phi_\pi^H) \\ &+ d\sigma_2 \cos 2\phi_\pi^H + d\Delta\sigma_2^- \sin(\phi_{S_A} - 2\phi_\pi^H) \\ &+ d\Delta\sigma_2^+ \sin(\phi_{S_A} + 2\phi_\pi^H). \end{aligned} \tag{28}$$

Equivalently, the numerator and denominator of the asymmetry will have the following expression:

$$\begin{aligned} d\sigma(\phi_{S_A}, \phi_\pi^H) - d\sigma(\phi_{S_A} + \pi, \phi_\pi^H) &\sim d\Delta\sigma_0 \sin\phi_{S_A} \\ &+ d\Delta\sigma_1^- \sin(\phi_{S_A} - \phi_\pi^H) + d\Delta\sigma_1^+ \sin(\phi_{S_A} + \phi_\pi^H) \\ &+ d\Delta\sigma_2^- \sin(\phi_{S_A} - 2\phi_\pi^H) + d\Delta\sigma_2^+ \sin(\phi_{S_A} + 2\phi_\pi^H), \end{aligned} \tag{29}$$

$$\begin{aligned} &d\sigma(\phi_{S_A}, \phi_\pi^H) + d\sigma(\phi_{S_A} + \pi, \phi_\pi^H) \\ &\quad \equiv 2d\sigma^{\text{unp}}(\phi_\pi^H) \sim d\sigma_0 + d\sigma_1 \cos\phi_\pi^H + d\sigma_2 \cos 2\phi_\pi^H. \end{aligned} \tag{30}$$

In terms of the polarized cross section, Eq. (28), we can define average values of appropriate circular functions of ϕ_{S_A} and ϕ_π^H, in order to single out the different contributions of interest:

$$\begin{aligned} &\langle W(\phi_{S_A}, \phi_\pi^H)\rangle(\boldsymbol{p}_{\text{j}}, z, k_{\perp\pi}) \\ &\quad = \frac{\int d\phi_{S_A} d\phi_\pi^H W(\phi_{S_A}, \phi_\pi^H) d\sigma(\phi_{S_A}, \phi_\pi^H)}{\int d\phi_{S_A} d\phi_\pi^H d\sigma(\phi_{S_A}, \phi_\pi^H)}. \end{aligned} \tag{31}$$

Alternatively, for the single-spin asymmetry we can, in close analogy with the case of semi-inclusive deeply inelastic scattering, define appropriate azimuthal moments,

$$A_N^{W(\phi_{S_A}, \phi_\pi^H)}(\boldsymbol{p}_{\text{j}}, z, k_{\perp\pi}) \equiv 2\langle W(\phi_{S_A}, \phi_\pi^H)\rangle(\boldsymbol{p}_{\text{j}}, z, k_{\perp\pi}) = 2\frac{\int d\phi_{S_A} d\phi_\pi^H W(\phi_{S_A}, \phi_\pi^H)[d\sigma(\phi_{S_A}, \phi_\pi^H) - d\sigma(\phi_{S_A} + \pi, \phi_\pi^H)]}{\int d\phi_{S_A} d\phi_\pi^H [d\sigma(\phi_{S_A}, \phi_\pi^H) + d\sigma(\phi_{S_A} + \pi, \phi_\pi^H)]}, \tag{32}$$

where $W(\phi_{S_A}, \phi_\pi^H)$ is again some appropriate circular function of ϕ_{S_A} and ϕ_π^H. In practice, it will be any of the circular functions appearing, e.g., in Eqs. (23) and (27) for specific partonic channels, and for polarized cross sections in general in Eq. (29) so that the coefficient related to the corresponding azimuthal moment is singled out.

III. PHENOMENOLOGY

In this section we will present and discuss some phenomenological implications of our approach for the unpolarized and single-transverse polarized cases in kinematical configurations accessible at RHIC by the STAR and PHENIX experiments. We will consider both central ($\eta_{\text{j}} = 0$) and forward ($\eta_{\text{j}} = 3.3$) (pseudo)rapidity configurations and different c.m. energies, $\sqrt{s} = 62.4$, 200, 500 GeV, aiming at a check of the potentiality of the approach in disentangling among different quark- and gluon-originating effects. We will also consider two very different situations concerning the TMD distribution and fragmentation functions involved.

We will first consider, for π^+ production only, a scenario in which the effects of all TMD functions are overmaximized. By this we mean that all TMD functions are maximized in size by imposing natural positivity bounds (and the Soffer bound for transversity [47,48]); moreover, the relative signs of all active partonic contributions are chosen so that they sum up additively. This very extreme scenario of course might imply the violation of other, more stringent, bounds and sum rules; examples are the Burkardt sum rule for the Sivers distribution [49], and the Schäfer-Teryaev sum rule for the Collins function [50]. On the other hand, it has the advantage of setting an upper bound on the absolute value of any of the effects playing a potential role in the azimuthal asymmetries. Therefore, all effects that are negligible or even marginal in this scenario may be directly discarded in subsequent refined phenomenological analyses.

As a second step in our study we will consider, for both neutral and charged pions, only the surviving effects, involving TMD functions for which parametrizations are available from independent fits to other spin and azimuthal asymmetries data in SIDIS, DY, and e^+e^- processes. Even if in our approach factorization and universality are not guaranteed for the process under consideration, we still believe that at the present stage this analysis can be of phenomenological relevance. It can certainly help in

pointing out inconsistencies among fits based on different processes, that could be a signal of universality-breaking effects. On the contrary, good consistency among fits to different observables from SIDIS, e^+e^-, and hadronic collisions data, while not proving factorization, might signal the smallness of possible universality-breaking terms and the usefulness of the factorization hypothesis in the present phenomenological analyses.

In this paper, for numerical calculations all TMD distribution and fragmentation functions will be taken in the simplified form where the functional dependencies on the parton light-cone momentum fraction and on transverse motion are completely factorized, assuming a Gaussian-like flavor-independent shape for the transverse momentum component. Preliminary lattice QCD calculations seem to support the validity of this assumption, see, e.g., Ref. [51]. Notice, however, that kinematical cuts introduced to prevent, as usual in the parton model, that the parton longitudinal momentum (energy) be opposite to (larger than) that of the parent hadron, effectively lead to a correlation between the light-cone momentum fraction and the transverse momentum, particularly at very small and very large ($\to 1$) light-cone momentum fractions (see, e.g., Appendix A of Ref. [42]).

For the generic parton a, the unpolarized and any of the polarized functions (that is, the Sivers and Boer-Mulders distributions and the Collins FF, and the analogous ones for gluons) will therefore assume, respectively, the forms $\mathcal{F}_a^{\rm unp}(u, p) = f_a^{\rm unp}(u) g^{(0)}(p)$ and $\Delta\mathcal{F}_a(u, p) = \Delta f_a(u) g^{(i)}(p)$, with $a = q, \bar{q}, g$, $i = 0, 1, 2, 3$, $u = x$ or z, and $p = k_\perp$ or $k_{\perp\pi}$ for distribution/fragmentation functions, respectively. Our parametrizations are required to respect angular momentum conservation in the forward direction, Eqs. (11) and (17); therefore, we define

$$g^{(i)}(p) = \left(\frac{p}{M}\right)^i h^{(i)}(p). \tag{33}$$

In particular, $g^{(0)}(p) \equiv g(p)$ is a simple Gaussian normalized to unity:

$$g^{(0)}(p) \equiv g(p) = \frac{1}{\pi\langle p_0^2\rangle} \exp[-p^2/\langle p_0^2\rangle], \tag{34}$$

while

$$g^{(i)}(p) = \left(\frac{p}{M}\right)^i h^{(i)}(p) = K_i \left(\frac{p}{M}\right)^i \exp[-p^2/\langle p_i^2\rangle], \quad i = 1, 2, 3. \tag{35}$$

All the polarized TMD functions are required to fulfill natural positivity bounds (for transversity, the Soffer bound) with respect to the corresponding unpolarized functions, coming from their general definition as

$$\frac{\mathcal{F}(S) - \mathcal{F}(-S)}{\mathcal{F}(S) + \mathcal{F}(-S)} = \frac{\Delta\mathcal{F}(S)}{n\mathcal{F}^{\rm unp}}, \tag{36}$$

where S is here the spin of the polarized quark or hadron involved, and $n = 1, 2$, depending on whether the polarized particle is, respectively, the final/initial one in the soft process considered (analogous relations hold for gluons). The positivity bound therefore reads:

$$\frac{|\Delta\mathcal{F}(u, p)|}{n\mathcal{F}^{\rm unp}(u, p)} \le 1 \quad \forall\ u, p. \tag{37}$$

As a matter of fact, to simplify relations we will consider a more conservative and stringent bound on the two factored components,

$$\frac{|\Delta f_a(u)|}{n f_a^{\rm unp}(u)} \le 1 \quad \forall\ u, \qquad \frac{g^{(i)}(p)}{g^{(0)}(p)} \le 1 \quad \forall\ p. \tag{38}$$

The first condition is usually fulfilled by defining

$$\Delta f_a(u) = n\mathcal{N}_a(u) f_a^{\rm unp}(u) = nN_a u^{\alpha_a}(1-u)^{\beta_a} \frac{(\alpha_a + \beta_a)^{(\alpha_a+\beta_a)}}{\alpha_a^{\alpha_a}\beta_a^{\beta_a}} f_a^{\rm unp}(u), \quad \text{with } |N_a| \le 1. \tag{39}$$

Concerning the transverse momentum–dependent component, $g^{(i)}(p)$, the positivity bound, Eq. (38), can only be fulfilled if, in Eq. (35), $\langle p_i^2\rangle < \langle p_0^2\rangle$. We then fix the factors K_i in Eq. (35) by saturating the bound at the maximum value of $g^{(i)}$. Finally, once a choice has been performed for $\langle p_0^2\rangle$, the $\langle p_i^2\rangle$'s are fixed by maximizing the corresponding $(i+1)$-th p moments. It is then an easy exercise to verify that this gives the conditions:

$$\langle p_1^2\rangle = \frac{2}{3}\langle p_0^2\rangle, \qquad \langle p_2^2\rangle = \frac{1}{2}\langle p_0^2\rangle, \qquad \langle p_3^2\rangle = \frac{2}{5}\langle p_0^2\rangle. \tag{40}$$

From the above equations it is clear that the overmaximized scenario for π^+ production we are going to present is obtained by taking, for all polarized TMD functions, the coefficients $\mathcal{N}_a(u) = 1$. For the transverse momentum component, the procedure delineated above guarantees the correct powerlike behavior in the forward direction, while maximizing the moments of the involved functions.

One also needs LO parametrizations for the usual unpolarized collinear distribution and fragmentation functions. Concerning the parton distribution functions, we will adopt the unpolarized set GRV98 [52] and (for the Soffer bound) the corresponding longitudinally polarized set GRSV2000 [53]. Since the range of the jet transverse momentum (the hard scale) covered is significant, we will take into account proper evolution with scale. Concerning transversity, in the maximized scenario we will fix it at the initial scale by saturating the Soffer bound and then letting it evolve. On the other hand, the transverse momentum component of all TMD functions is kept fixed with no

evolution with scale. Notice that at this stage evolution properties of the full TMD functions are not known.

As for fragmentation functions, we will adopt two well-known LO sets among those available in the literature: the set by Kretzer (K) [54] and the one by De Florian, Sassot, and Stratmann (DSS) [55]. Our choice is dictated by the subsequent use of the two available parametrization sets for the Sivers and Collins functions in our scheme, that have been derived in the past years by adopting these sets of FFs. Let us notice that, as the authors of Ref. [55] suggest, the LO DSS fragmentation function set has to be handled with some care. In fact, aiming at reproducing for the first time unpolarized cross sections for inclusive hadronic collisions, at LO accuracy a very huge gluon component (as compared to other FF sets) is required. This could be an artifact of the LO set, which in fact is sizably reduced in the NLO parametrizations. However, we are at present forced to work at leading order in our TMD approach. The comparison among the two sets adopted will allow us to stress the possible effects of the large gluon component in the LO DSS set.

Concerning the parametrizations of the transversity and Sivers distributions and of the Collins functions, we will consider two sets resulting from the fits to available data on azimuthal asymmetries in polarized SIDIS from HERMES and COMPASS experiments, and on hadron-pair production in e^+e^- collisions from Belle. Set 1 (SIDIS 1) includes the u, d quark Sivers functions of Ref. [56], the u, d quark transversity distributions, and the favored and unfavored Collins FFs of Ref. [57]. Data include preliminary HERMES data for charged pions [58] and COMPASS data on charged hadrons with a deuteron target [59] on the SIDIS Sivers asymmetry; HERMES data for charged pions [11,60] and COMPASS data for charged hadrons with a deuteron target [61] on the SIDIS Collins asymmetry; and early Belle data on azimuthal asymmetries for hadron-pair production in e^+e^- collisions [14]. No SIDIS data on kaons were used and the Kretzer set [54] for pion FFs was used. Set 2 (SIDIS 2) includes the new u, d, and sea-quark Sivers functions of Ref. [62] and an updated set of the u, d quark transversity distributions and of the favored and unfavored Collins FFs of Ref. [63]. Corresponding data include: preliminary HERMES data on pions and charged kaons [64] and preliminary COMPASS data on charged pions and kaons with a deuteron target [65] for the SIDIS Sivers asymmetry; preliminary HERMES data for pions [64] and COMPASS data for charged pions with a deuteron target [12] on the SIDIS Collins asymmetry; recent Belle data on azimuthal asymmetries for hadron-pair production in e^+e^- collisions [15]; the DSS set [55] for pion and kaon FFs was adopted.

Notice that the almost unknown gluon Sivers function was tentatively taken positive and saturated to an updated version of the bound obtained in Ref. [66] by considering PHENIX data for the π^0 transverse SSA at midrapidity production in polarized pp collisions at RHIC [67].

It is also important to stress here that polarized SIDIS data on azimuthal asymmetries from HERMES and COMPASS experiments cover a relatively limited range of Bjorken x, $x_B \leq 0.3$. Therefore, the statistical uncertainty of the parametrizations available for the transversity and Sivers distributions is huge at large x values, where one extrapolates their behavior. As we will see, this reflects in the very different behavior of the Sivers and Collins asymmetries when estimated adopting sets SIDIS 1 and SIDIS 2, respectively.

Finally, regarding the quark Boer-Mulders distribution function, much less is known and available parametrizations have large uncertainties. In our calculations we have adopted the recent parametrization by Barone, Melis, and Prokudin (BMP) [68], which makes use of our set SIDIS 2 for the transversity and Sivers distributions and for the Collins function.

We have considered the following kinematical configurations for the PHENIX and STAR experiments at RHIC:

(1) $\sqrt{s} = 62.4$ GeV, $\eta_j = 0$, $1 \leq p_{jT} \leq 14$ GeV;
(2) At $\sqrt{s} = 62.4$ GeV, the forward rapidity configuration covers a very limited range of p_{jT} values, which probably prevents the unambiguous definition of jets and leading particles, therefore we will not consider it in the sequel;
(3) $\sqrt{s} = 200$ GeV, $\eta_j = 0$, $2 \leq p_{jT} \leq 15$ GeV;
(4) $\sqrt{s} = 200$ GeV, $\eta_j = 3.3$, $2 \leq p_{jT} \leq 6.5$ GeV $[0.27 \leq x_F \leq 0.88]$;
(5) $\sqrt{s} = 500$ GeV, $\eta_j = 0$, $2 \leq p_{jT} \leq 15$ GeV;
(6) $\sqrt{s} = 500$ GeV, $\eta_j = 3.3$, $2 \leq p_{jT} \leq 15$ GeV $[0.11 \leq x_F \leq 0.81]$.

For completeness, in the forward rapidity case we have also shown the range of x_F covered, where x_F is the usual Feynman variable for the jet, $x_F = 2p_{jL}/\sqrt{s}$.

In all cases considered, since we are interested in azimuthal asymmetries for leading particles inside the jet, we will present results obtained by integrating the light-cone momentum fraction of the observed hadron, z, in the range $z \geq 0.3$.

A. Azimuthal asymmetries for the unpolarized cross section

In this section we will discuss results for the azimuthal $\langle \cos\phi_\pi^H \rangle$, $\langle \cos 2\phi_\pi^H \rangle$ asymmetries [see Eq. (31)] in the unpolarized cross section for the process $pp \to \text{jet} + \pi + X$.

As it is easy to verify by looking, e.g., at Eqs. (21) and (26) for the $qq \to qq$ and $gg \to gg$ partonic contributions (analogous results, where allowed, hold for all other channels), in the unpolarized case:

(1) The symmetric part gets contributions by the usual unpolarized term, already present in the collinear approach, and by an additional term involving a Boer-Mulders⊗Boer-Mulders convolution for the initial quarks (or the analogous terms involving linearly polarized gluons); however, we have explicitly

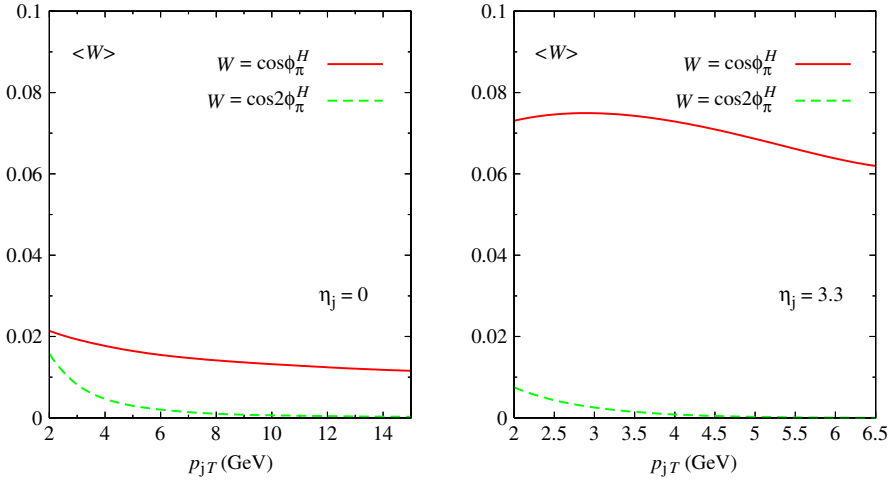

FIG. 2 (color online). Maximized quark-originated ($\cos\phi_\pi^H$) and gluon-originated ($\cos 2\phi_\pi^H$) asymmetries (solid red and dashed green lines, respectively) for the unpolarized $pp \to \text{jet} + \pi^+ + X$ process, at $\sqrt{s} = 200$ GeV c.m. energy in the central (left panel) and forward (right panel) rapidity regions as a function of p_{jT}, from $p_{jT} = 2$ GeV up to the maximum allowed value, adopting the Kretzer FF set. Slightly lower (similar) values are obtained for quark (gluon) asymmetries when using the DSS set.

checked that even in the maximized scenario this last contribution is always negligible in all the kinematical configurations considered; therefore, we will not discuss it anymore in the sequel;

(2) The $\cos\phi_\pi^H$ asymmetry is generated by the quark Boer-Mulders⊗Collins convolution term, involving a transversely polarized quark and an unpolarized hadron both in the initial state and in the fragmentation process. In the central rapidity region ($\eta_j = 0$) the maximized value of this asymmetry is of the order 1–3%, depending on the fragmentation function set adopted and on the c.m. energy considered, being almost negligible at $\sqrt{s} = 500$ GeV. In the forward rapidity region, $\eta_j = 3.3$, the maximized $\cos\phi_\pi^H$ asymmetry can be much larger both at $\sqrt{s} = 200$ and 500 GeV. As an example, in Fig. 2 we show the maximized $\cos\phi_\pi^H$ asymmetry (solid red lines) for π^+ production at c.m. energy $\sqrt{s} = 200$ GeV in the central (left panel) and forward (right panel) rapidity regions as a function of p_{jT}, from $p_{jT} = 2$ GeV up to the maximum allowed value, adopting the Kretzer FF set. Slightly lower values are obtained using the DSS set.

(3) The $\cos 2\phi_\pi^H$ asymmetry is related to the term involving linearly polarized gluons and unpolarized hadrons both in the initial state and in the fragmentation process, that is, the convolution of a Boer-Mulders-like gluon distribution with a Collins-like gluon FF. Even the maximized contribution is practically negligible in the kinematical configurations considered. As an example, again in Fig. 2, we show the maximized $\cos 2\phi_\pi^H$ asymmetry (dashed green lines) for π^+ production at $\sqrt{s} = 200$ GeV c.m. energy in the central (left panel) and forward (right panel) rapidity regions as a function of p_{jT}, adopting the Kretzer FF set. Similar results are obtained using the DSS set.

Concerning results with available parametrizations, for the quark-originated $\cos\phi_\pi^H$ asymmetry we have verified that the asymmetries obtained with the parametrizations adopted here, our set SIDIS 2 and the BMP set for the Boer-Mulders function, are negligible in all kinematical configurations considered. No parametrizations are presently available for the analogous gluon contributions leading to the $\cos 2\phi_\pi^H$ asymmetry.

B. Azimuthal asymmetries for $A_N(p^\uparrow p \to \text{jet} + \pi + X)$

Let us now discuss our numerical results for the Sivers ($A_N^{\sin\phi_{S_A}}$) asymmetry and the quark [$A_N^{\sin(\phi_{S_A} \mp \phi_\pi^H)}$] and gluon [$A_N^{\sin(\phi_{S_A} \mp 2\phi_\pi^H)}$] Collins(-like) asymmetries; see Eq. (32). Our estimates are qualitatively similar at the three different c.m. energies considered, with some differences in the size of the asymmetries and in the relative weight of the quark and gluon contributions where both play a role. Therefore, we will concentrate on the results obtained at $\sqrt{s} = 200$ GeV.

1. The Sivers asymmetry

In this case, both quark and gluon contributions can be present, and they cannot be disentangled. However, some kinematical configurations can be dominated by quark or gluon terms, and a sizable asymmetry in these regions might be an unambiguous indication for a Sivers asymmetry generated by the dominant partonic contribution.

In Fig. 3 we show the total observable Sivers asymmetry (solid red line) and the corresponding quark and gluon contributions (dashed green and dotted blue lines,

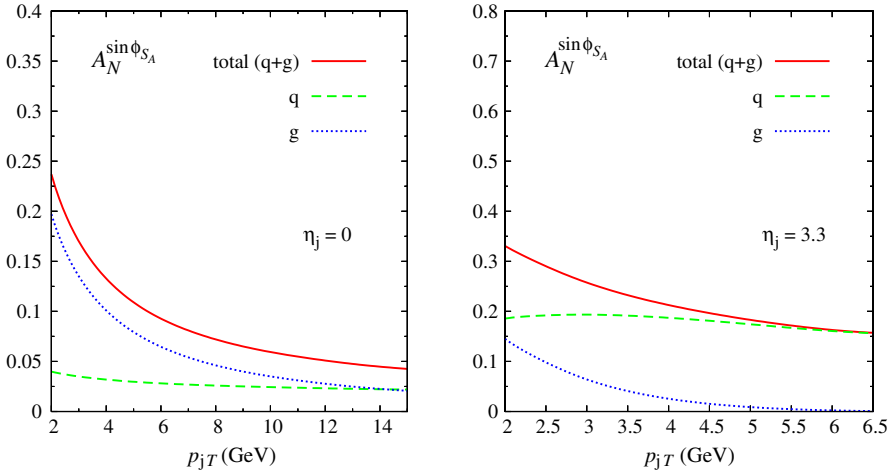

FIG. 3 (color online). Maximized total (solid red line), quark-originated (dashed green line) and gluon-originated (dotted blue line) Sivers asymmetry for the $p^\uparrow p \to \text{jet} + \pi^+ + X$ process, at $\sqrt{s} = 200$ GeV c.m. energy in the central (left panel) and forward (right panel) rapidity regions as a function of p_{jT}, from $p_{jT} = 2$ GeV up to the maximum allowed value, adopting the Kretzer FF set. Similar results with some differences in the total size and in the relative weight of the quark and gluon contributions are obtained adopting the DSS set of fragmentation functions and considering different c.m. energies.

respectively) for π^+ production, in the maximized scenario and adopting the Kretzer fragmentation function set, at $\sqrt{s} = 200$ GeV and as a function of p_{jT} in the central (left panel) and forward (right panel) rapidity regions. The maximized potential Sivers asymmetry can be very large in both cases. In the central rapidity region, the asymmetry is dominated by the gluon contribution at the lowest p_{jT} range while gets comparable quark and gluon contributions in the large p_{jT} range. A large Sivers asymmetry around $p_{jT} = 4$–6 GeV could then be a clear indication for a sizable gluon contribution. However, one must not forget that, as mentioned above, recent PHENIX results for $A_N(p^\uparrow p \to \pi^0 + X)$ in the central rapidity region put much more stringent bounds on the gluon Sivers distribution than the simple positivity bound adopted in the maximized scenario. We have checked that even adopting this more stringent bound, a potential gluon-generated Sivers asymmetry of the order of 2% might survive in this region, being possibly measurable. In the forward rapidity region, on the contrary, the quark and gluon contributions are comparable at low p_{jT} values, while the maximized asymmetry is dominated by the quark contribution for $p_{jT} \gtrsim 4$ GeV. Therefore, a large Sivers asymmetry in this kinematical range could be ascribed unambiguously to the quark Sivers effect. Qualitatively similar results are obtained at the other c.m. energies considered or adopting the DSS set of fragmentation functions, with some changes in the total size and in the relative weights of the quark and gluon contributions.

In Fig. 4 we show, for both neutral and charged pions, the quark and gluon contributions to the Sivers asymmetry, obtained by adopting, respectively, the parametrization sets SIDIS 1 (quark contribution: solid red line; gluon contribution: dashed green line) and SIDIS 2 (quark contribution: dotted blue line; gluon contribution: dot-dashed cyan line), and the updated version of the bound on the gluon Sivers function derived in Ref. [66], at $\sqrt{s} = 200$ GeV and in the forward rapidity region, as a function of p_{jT}. The dotted black vertical line delimits the region beyond which the SIDIS parametrizations for the quark Sivers distribution are extrapolated outside the x_B region covered by SIDIS data and are therefore plagued by large uncertainties. This reflects on the fact that below this limit the two sets give comparable results, while above it they differ remarkably. In particular, at the largest reachable p_{jT} values the SIDIS 1 set gives a Sivers asymmetry of the order 2–4%, while the SIDIS 2 set leads to a negligible asymmetry. Therefore, a measurement of this asymmetry might help in clarifying the behavior of the quark Sivers distribution in the large x region, which is not covered by present SIDIS data from HERMES and COMPASS experiments. Future planned measurements at the Jefferson Lab (JLab) 12 GeV Upgrade will also be very useful in this respect (see, e.g., Ref. [69]).

2. The Collins $A_N^{\sin(\phi_{S_A} \mp \phi_\pi^H)}$ and the Collins-like $A_N^{\sin(\phi_{S_A} \mp 2\phi_\pi^H)}$ asymmetries

Let us first briefly discuss the quark-generated asymmetry $A_N^{\sin(\phi_{S_A} + \phi_\pi^H)}$. It comes from two distinct contributions—see, e.g., Eq. (23)—for the $qq \to qq$ channel: one involving the convolution between the term of the TMD transversity distribution suppressed in the collinear configuration ($\propto k_{\perp q}^2 h_{1T}^{\perp q}$) and the Collins function; another term involving the convolution of the Sivers and Boer-Mulders distributions for the initial quarks with the

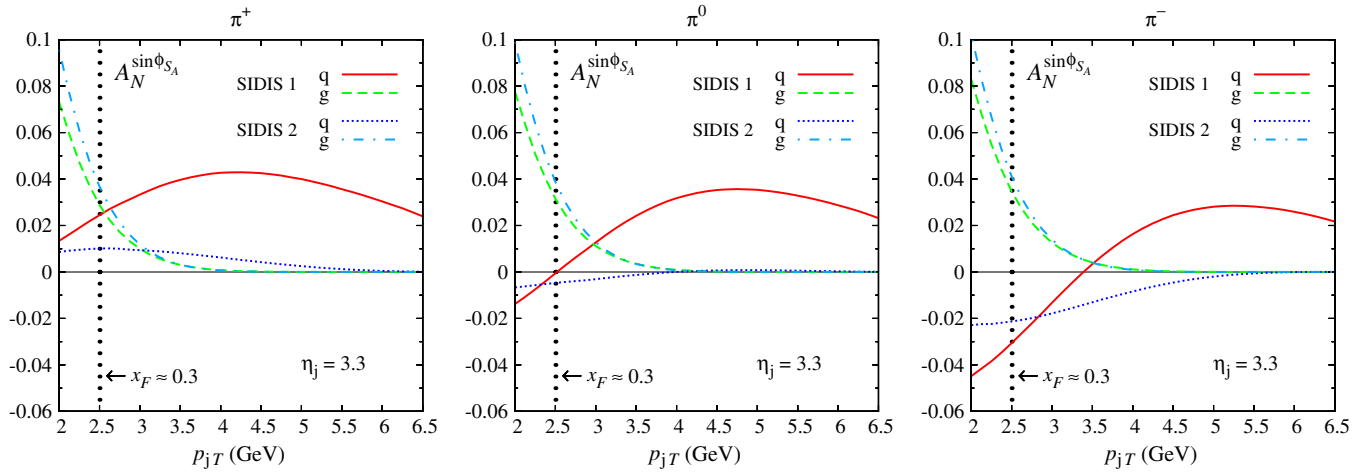

FIG. 4 (color online). The estimated quark and gluon contributions to the Sivers asymmetry for the $p^\uparrow p \to \text{jet} + \pi + X$ process, obtained adopting, respectively, the parametrization sets SIDIS 1 (quark contribution: solid red line; gluon contribution: dashed green line) and SIDIS 2 (quark contribution: dotted blue line; gluon contribution: dot-dashed cyan line), at $\sqrt{s} = 200$ GeV c.m. energy in the forward rapidity region and as a function of p_{jT}, from $p_{jT} = 2$ GeV up to the maximum allowed value. The dotted black vertical line delimits the region beyond which the SIDIS parametrizations for the quark Sivers function are presently plagued by large uncertainties. Similar results are obtained when considering different c.m. energies.

Collins function for the final quark [an analogous term appears also in the $A_N^{\sin(\phi_{S_A} - \phi_\pi^H)}$ asymmetry; see Eq. (23)]. We have explicitly checked that for the process under study and the kinematical configurations considered both these contributions are always negligible already in the maximized scenario. Therefore we will not consider the $\sin(\phi_{S_A} + \phi_\pi^H)$ asymmetry in the sequel. A similar situation holds also for the gluon-generated $A_N^{\sin(\phi_{S_A} + 2\phi_\pi^H)}$ asymmetry, where two contributions analogous to the quark ones discussed above but for linearly polarized gluons are involved.

In Fig. 5 we present the quark $A_N^{\sin(\phi_{S_A} - \phi_\pi^H)}$ Collins asymmetry (solid red lines) and the gluon $A_N^{\sin(\phi_{S_A} - 2\phi_\pi^H)}$ Collins-like asymmetry (dashed green lines) in the maximized scenario for the $p^\uparrow p \to \text{jet} + \pi^+ + X$ process, at $\sqrt{s} = 200$ GeV c.m. energy in the central (left panel) and forward (right panel) rapidity regions as a function of p_{jT}, from $p_{jT} = 2$ GeV up to the maximum allowed value, adopting the Kretzer FF set. In the central rapidity region the quark Collins asymmetry is very small at the lowest p_{jT} values, then increases almost linearly, reaching about 8% at the upper range. At $\sqrt{s} = 500(62.4)$ GeV c.m. energy the behavior is similar and the largest reached size, at large p_{jT} values, is about half (twice), respectively. Results with the DSS fragmentation function set are slightly lower in size. Instead, in the forward rapidity region the asymmetry is (potentially) always large and increases almost linearly from about 25% to about 70% going from the lowest to the largest p_{jT} values. Results are very similar at $\sqrt{s} = 500$ GeV and when adopting the DSS fragmentation function set.

Concerning the gluon Collins-like asymmetry, both in the central and in the forward rapidity regions it is of the order of 5% at the lowest p_{jT} values, then starts decreasing slowly and becomes negligible at large p_{jT} values. Very similar results hold at different energies and when adopting the DSS set.

Let us now consider, for both neutral and charged pions, numerical results for the quark Collins asymmetry obtained adopting the parametrizations SIDIS 1 and SIDIS 2 for the transversity distribution and the Collins fragmentation function (no parametrizations are available yet in the analogous gluon case). It turns out that in the central rapidity region the estimated asymmetry is practically negligible in all cases considered (different c.m. energies and FF sets). For the SIDIS 2 parametrization and at $\sqrt{s} = 62.4$ GeV the asymmetry for charged pions can reach about 2–3% in size at large p_{jT} values.

Concerning the forward rapidity region, in Fig. 6 we present, for both charged and neutral pions, some results at $\sqrt{s} = 200$ GeV c.m. energy as a function of p_{jT}, adopting the SIDIS 1 (left panel) and the SIDIS 2 (right panel) parametrizations. The Collins asymmetry for neutral pions (dashed green lines) turns out to be practically negligible. This can be easily understood since in the available parametrizations the favored (e.g., $u \to \pi^+$) and unfavored (e.g., $d \to \pi^+$) Collins fragmentation functions are comparable in size and opposite in sign. Because of isospin symmetry the π^0 FFs are half the sum of those for charged pions, therefore the π^0 Collins FF is always very small. Moreover, the u, d quark transversity distributions are also opposite in sign, leading to additional cancellations among quark contributions. For charged pions, similarly to the case of the Sivers asymmetry, the two parametrizations

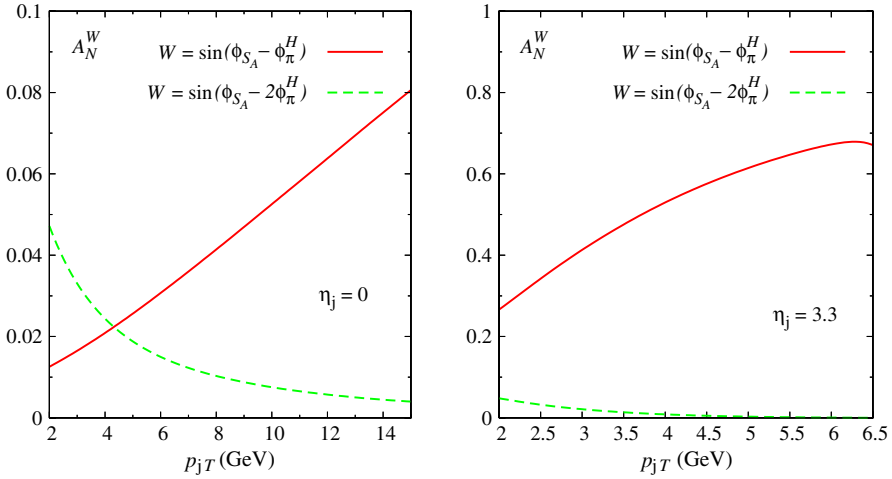

FIG. 5 (color online). Maximized quark (solid red line) and gluon (dashed green line) Collins(-like) asymmetries for the $p^\uparrow p \to$ jet $+ \pi^+ + X$ process, at $\sqrt{s} = 200$ GeV c.m. energy in the central (left panel) and forward (right panel) rapidity regions as a function of p_{jT}, from $p_{jT} = 2$ GeV up to the maximum allowed value, adopting the Kretzer FF set. Notice the difference in scale between the two panels. Similar results, with some differences in the total size and in the relative weight of the quark and gluon contributions are obtained adopting the DSS set of fragmentation functions and considering different c.m. energies.

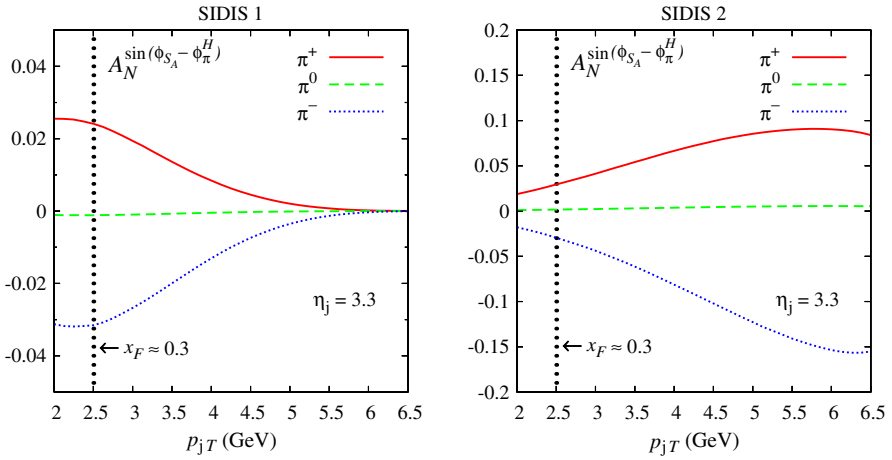

FIG. 6 (color online). The estimated quark Collins asymmetry for the $p^\uparrow p \to$ jet $+ \pi + X$ process, obtained adopting the parametrizations SIDIS 1 (left panel) and SIDIS 2 (right panel), respectively, at $\sqrt{s} = 200$ GeV c.m. energy in the forward rapidity region and as a function of p_{jT}, from $p_{jT} = 2$ GeV up to the maximum allowed value. Notice the difference in scale between the two panels. The dotted black vertical line delimits the region beyond which the SIDIS parametrizations for the quark transversity distribution are presently plagued by large uncertainties. Similar results are obtained when considering different c.m. energies.

give comparable results (notice the different scale adopted in the two panels) in the p_{jT} region where the transversity distribution is reasonably constrained by SIDIS data (see the dotted black vertical line), while they lead to completely different estimates in the large p_{jT} region where the parametrizations are basically unconstrained by SIDIS data. In particular, in this region the SIDIS 1 set gives almost negligible results, while the SIDIS 2 set leads to an asymmetry of about 8% (π^+) and 15% (π^-) in size, which should be hopefully measurable. A measurement of this asymmetry would be then very important and helpful in clarifying the large x behavior of the quark transversity distribution. A qualitatively similar situation is obtained at $\sqrt{s} = 500$ GeV.

3. Transverse single-spin asymmetry for inclusive jet production

For completeness we have extended our analysis to the transverse single-spin asymmetry for inclusive jet production in polarized pp collisions, $A_N(p^\uparrow p \to \text{jet} + X)$. In principle, this case can be obtained by the jet + pion production process by integrating over the full pion phase space. Of course, in this case the unobserved fragmentation

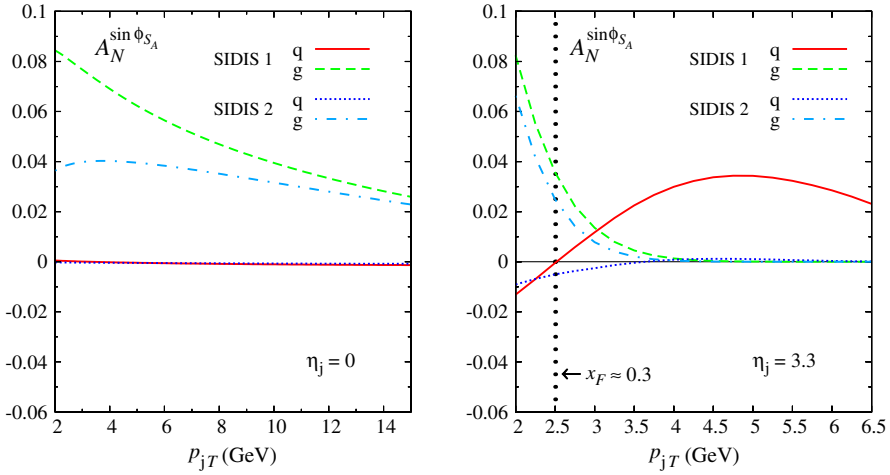

FIG. 7 (color online). The estimated quark and gluon Sivers contributions to the transverse single-spin asymmetry for the $p^{\uparrow}p \rightarrow \text{jet} + X$ process, at $\sqrt{s} = 200$ GeV c.m. energy in the central (left panel) and forward (right panel) rapidity regions as a function of p_{jT}, from $p_{jT} = 2$ GeV up to the maximum allowed value, obtained adopting the parametrization sets SIDIS 1 (quark contribution: solid red line; gluon contribution: dashed green line) and SIDIS 2 (quark contribution: dotted blue line; gluon contribution: dot-dashed cyan line). The dotted black vertical line in the right panel delimits the region beyond which the SIDIS parametrizations for the quark transversity distribution are presently plagued by large uncertainties. Similar results with some differences in the total size and in the relative weight of the quark and gluon contributions are obtained considering different c.m. energies.

process in the final state plays no role in the azimuthal asymmetries, which can only be originated by mechanisms, like the Sivers effect, acting in the initial state. Moreover, we have verified that for the kinematical configurations considered in this paper all contributions but the Sivers effect play a negligible role already in the maximized scenario. Therefore, in what follows, we limit our discussion to the Sivers asymmetry. As already mentioned, in this case quark and gluon contributions cannot be disentangled since they add up, leading to a $\sin\phi_{S_A}$ asymmetry.

Let us first discuss the maximized scenario. In the central rapidity region, the maximized gluon contribution is of the order 20% at the lowest p_{jT} values, decreasing fast to about 3% at large p_{jT} for all c.m. energies considered. The maximized quark contribution is of the order 1–3% in the full p_{jT} range, slowly decreasing with the increase of the c.m. energy. The total potential effect is therefore sizable only at small p_{jT} values due to the gluon component. The situation is different in the forward rapidity region. Here both quark and gluon maximized contributions can be very sizable, showing as expected an opposite, respectively, increasing and decreasing, behavior versus p_{jT}. The total maximized Sivers effect is therefore large in the full p_{jT} range with little dependence on the c.m. energy.

Concerning numerical estimates obtained adopting the available parametrizations SIDIS 1 and SIDIS 2 for the quark Sivers function, and the updated bound on the gluon Sivers function, the situation is the following:

(1) In the central rapidity region, for both SIDIS 1,2 sets and all energies considered the quark contribution is practically negligible. Instead, the gluon contribution can be at most of the order 10–15% at the lowest p_{jT} values but decreases quickly with the increasing of p_{jT}. However, at least for $\sqrt{s} = 200$ and 500 GeV, it can still be about 2–4% in the upper p_{jT} range. The measurement of a comparable Sivers asymmetry in these kinematical configurations could then be a clear indication for a gluonic contribution to the Sivers effect.

(2) In the forward rapidity region the quark contribution is small and negative at $p_{jT} = 2$ GeV for both sets adopted, while at large p_{jT} values it is negligible for the SIDIS 2 set and positive and of the order 2–4% for the SIDIS 1 set. The gluon contribution can be sizable at very low p_{jT} values but becomes negligible quickly as p_{jT} increases.

As an example, in Fig. 7 we show the estimated quark and gluon Sivers contributions to the transverse single-spin asymmetry for inclusive jet production in the central (left panel) and forward (right panel) rapidity regions at $\sqrt{s} = 200$ GeV, obtained adopting the SIDIS 1 and SIDIS 2 parametrizations for the quark Sivers function and the updated bound for the gluon Sivers function (assumed to be positive).

IV. CONCLUSIONS

In this paper we have presented a study of the azimuthal asymmetries measurable in the distribution of leading unpolarized or spinless hadrons (mainly pions) inside a

large-p_T jet produced in unpolarized and single-transverse polarized proton-proton collisions for kinematical configurations accessible at RHIC. To this end, we have adopted a generalized TMD parton model approach with inclusion of spin and intrinsic parton motion effects both in the distribution and in the fragmentation sectors. We have shown how a detailed phenomenological analysis of these effects can be very useful in shedding light on several aspects of azimuthal and transverse single-spin asymmetries in (un) polarized hadronic collisions. It may also help in clarifying the role played by the quark (gluon) Sivers distribution and by the Collins(-like) fragmentation function in the sizable single-spin asymmetries observed at RHIC for forward pion production. Available parametrizations for the TMD quark transversity and Sivers distribution functions, obtained by fitting SIDIS and e^+e^- data, are presently largely unconstrained for light-cone momentum fractions $x \geq 0.3$, that is, the region playing a fundamental role for forward pion production at RHIC. The transverse single-spin asymmetry for inclusive particle production is a complicated higher-twist effect involving several TMD mechanisms that cannot be easily disentangled as in the case of SIDIS and DY processes. On the contrary, the leading-twist azimuthal asymmetries discussed in this paper allow one, in close analogy with the SIDIS case, to discriminate among different effects by taking suitable moments of the asymmetries. Moreover, we have shown that in principle quark and gluon originating jets can be distinguished, at least in some kinematical regimes. Neglecting intrinsic motion in the distribution sector leaves at work only the Collins azimuthal asymmetry. As already shown by Yuan [41], the measurements proposed in this paper would allow one to determine unambiguously the role played by the Collins effect. Universality properties of the Collins function have been proved, so that this process can be complementary to the SIDIS and e^+e^- measurements in order to constrain the quark Collins fragmentation function and, as an important by-product, the large x behavior of the TMD transversity distribution function.

For the quark and gluon Sivers function and for the Boer-Mulders function the situation is more complicated. Since factorization has not been proven yet for inclusive particle production in hadronic collisions, the use, based on universality, of the parametrizations obtained by fitting SIDIS and e^+e^- data might be questionable. The phenomenological analysis proposed in this paper gives us the opportunity of testing the factorization and universality assumptions, and of gaining information on the size and *sign* of the TMD functions discussed. This can be very useful also for further developments of the TMD approach, since it is difficult *a priori* to assess at which values of the factorization scale the role and the size of possible factorization-breaking terms become relevant and non-negligible.

Let us finally stress again that the unambiguous measurement of any of the asymmetries, other than the Collins one, discussed in this paper would be a clear indication of the role played by intrinsic parton motion in the initial colliding hadrons for the spin asymmetry sector in polarized hadronic collisions.

ACKNOWLEDGMENTS

We are grateful to Pietro Contu and Mattia Melis for collaboration during the early stages of this work. C. P. is supported by Regione Autonoma della Sardegna (RAS) through a research grant under the PO Sardegna FSE 2007-2013, L.R. 7/2007, "Promozione della ricerca scientifica e dell'innovazione tecnologica in Sardegna." U. D. and F. M. acknowledge partial support by Italian Ministero dell'Istruzione, dell'Università e della Ricerca Scientifica (MIUR) under Cofinanziamento Progetti di Rilevante Interesse Nazionale (PRIN 2008), and by the European Community under the FP7 "Integrating Activities" project, "Study of Strongly Interacting Matter" (HadronPhysics2), Grant Agreement No. 227431.

[1] U. D'Alesio and F. Murgia, Prog. Part. Nucl. Phys. **61**, 394 (2008).
[2] V. Barone, F. Bradamante, and A. Martin, Prog. Part. Nucl. Phys. **65**, 267 (2010).
[3] D. L. Adams *et al.* (E704 Collaboration), Phys. Lett. B **264**, 462 (1991).
[4] D. L. Adams *et al.* (E581-E704 Collaboration), Z. Phys. C **56**, 181 (1992).
[5] J. Adams *et al.* (STAR Collaboration), Phys. Rev. Lett. **92**, 171801 (2004).
[6] B. I. Abelev *et al.* (STAR Collaboration), Phys. Rev. Lett. **101**, 222001 (2008).
[7] K. J. Heller, in *Proceedings of the 12th International Symposium on High-Energy Spin Physics, Amsterdam, The Netherlands,* edited by C. W. de Jager *et al.* (World Scientific, Singapore, 1997).
[8] L. Y. Zhu *et al.* (FNAL-E866/NuSea Collaboration), Phys. Rev. Lett. **99**, 082301 (2007).
[9] L. Y. Zhu *et al.* (FNAL-E866/NuSea Collaboration), Phys. Rev. Lett. **102**, 182001 (2009).
[10] A. Airapetian *et al.* (HERMES Collaboration), Phys. Rev. Lett. **103**, 152002 (2009).
[11] L. L. Pappalardo (HERMES Collaboration), Eur. Phys. J. A **38**, 145 (2008).
[12] M. Alekseev *et al.* (COMPASS Collaboration), Phys. Lett. B **673**, 127 (2009).
[13] M. G. Alekseev *et al.* (COMPASS Collaboration), Phys. Lett. B **692**, 240 (2010).

[14] K. Abe *et al.* (Belle Collaboration), Phys. Rev. Lett. **96**, 232002 (2006).
[15] R. Seidl *et al.* (Belle Collaboration), Phys. Rev. D **78**, 032011 (2008).
[16] B. I. Abelev *et al.* (STAR Collaboration), Phys. Rev. D **80**, 111108 (2009).
[17] S. S. Adler *et al.* (PHENIX Collaboration), Phys. Rev. Lett. **91**, 241803 (2003).
[18] A. V. Efremov and O. V. Teryaev, Phys. Lett. B **150**, 383 (1985).
[19] J. Qiu and G. Sterman, Phys. Rev. Lett. **67**, 2264 (1991).
[20] J. Qiu and G. Sterman, Phys. Rev. D **59**, 014004 (1998).
[21] L. Gamberg and Z. B. Kang, Phys. Lett. B **696**, 109 (2011).
[22] D. Boer, P. J. Mulders, and F. Pijlman, Nucl. Phys. **B667**, 201 (2003).
[23] J. C. Collins and A. Metz, Phys. Rev. Lett. **93**, 252001 (2004).
[24] J. Collins, arXiv:0708.4410.
[25] J. Collins and J. W. Qiu, Phys. Rev. D **75**, 114014 (2007).
[26] C. J. Bomhof and P. J. Mulders, Nucl. Phys. **B795**, 409 (2008).
[27] T. C. Rogers and P. J. Mulders, Phys. Rev. D **81**, 094006 (2010).
[28] X. Ji and F. Yuan, Phys. Lett. B **543**, 66 (2002).
[29] A. V. Belitsky, X. Ji, and F. Yuan, Nucl. Phys. **B656**, 165 (2003).
[30] X. Ji, J. P. Ma, and F. Yuan, Phys. Rev. D **71**, 034005 (2005).
[31] X. Ji, J. P. Ma, and F. Yuan, Phys. Lett. B **597**, 299 (2004).
[32] X. Ji, J. W. Qiu, W. Vogelsang, and F. Yuan, Phys. Rev. Lett. **97**, 082002 (2006).
[33] X. Ji, J. W. Qiu, W. Vogelsang, and F. Yuan, Phys. Rev. D **73**, 094017 (2006).
[34] X. Ji, J. W. Qiu, W. Vogelsang, and F. Yuan, Phys. Lett. B **638**, 178 (2006).
[35] D. W. Sivers, Phys. Rev. D **41**, 83 (1990).
[36] D. W. Sivers, Phys. Rev. D **43**, 261 (1991).
[37] D. Boer and P. J. Mulders, Phys. Rev. D **57**, 5780 (1998).
[38] J. C. Collins, Nucl. Phys. **B396**, 161 (1993).
[39] M. Anselmino *et al.*, Phys. Rev. D **73**, 014020 (2006).
[40] U. D'Alesio, *"Transverse Momentum, Spin, and Position Distributions of Partons in Hadrons,"* ECT*, Trento, Italy, 2007 (unpublished).
[41] F. Yuan, Phys. Rev. Lett. **100**, 032003 (2008).
[42] U. D'Alesio and F. Murgia, Phys. Rev. D **70**, 074009 (2004).
[43] M. Anselmino, M. Boglione, U. D'Alesio, E. Leader, and F. Murgia, Phys. Rev. D **71**, 014002 (2005).
[44] P. J. Mulders and R. D. Tangerman, Nucl. Phys. **B461**, 197 (1996).
[45] F. Yuan, Phys. Rev. D **77**, 074019 (2008).
[46] F. Yuan, Phys. Lett. B **666**, 44 (2008).
[47] J. Soffer, Phys. Rev. Lett. **74**, 1292 (1995).
[48] A. Bacchetta, M. Boglione, A. Henneman, and P. J. Mulders, Phys. Rev. Lett. **85**, 712 (2000).
[49] M. Burkardt, Phys. Rev. D **69**, 091501 (2004).
[50] A. Schäfer and O. V. Teryaev, Phys. Rev. D **61**, 077903 (2000).
[51] P. Hägler, Phys. Rep. **490**, 49 (2010).
[52] M. Glück, E. Reya, and A. Vogt, Eur. Phys. J. C **5**, 461 (1998).
[53] M. Glück, E. Reya, M. Stratmann, and W. Vogelsang, Phys. Rev. D **63**, 094005 (2001).
[54] S. Kretzer, Phys. Rev. D **62**, 054001 (2000).
[55] D. de Florian, R. Sassot, and M. Stratmann, Phys. Rev. D **75**, 114010 (2007).
[56] M. Anselmino *et al.*, Phys. Rev. D **72**, 094007 (2005).
[57] M. Anselmino *et al.*, Phys. Rev. D **75**, 054032 (2007).
[58] M. Diefenthaler (HERMES Collaboration), AIP Conf. Proc. **792**, 933 (2005).
[59] V. Y. Alexakhin *et al.* (COMPASS Collaboration), Phys. Rev. Lett. **94**, 202002 (2005).
[60] A. Airapetian *et al.* (HERMES Collaboration), Phys. Rev. Lett. **94**, 012002 (2005).
[61] E. S. Ageev *et al.* (COMPASS Collaboration), Nucl. Phys. **B765**, 31 (2007).
[62] M. Anselmino *et al.*, Eur. Phys. J. A **39**, 89 (2009).
[63] M. Anselmino *et al.*, Nucl. Phys. B, Proc. Suppl. **191**, 98 (2009).
[64] M. Diefenthaler (HERMES Collaboration), *Proceedings of the 15th International Workshop on Deep Inelastic Scattering (DIS 2007), Munich, Germany, 2007*, edited by G. Grindhammer and K. Sachs (ScienceWise Publishing, Berlin, 2007).
[65] A. Martin (COMPASS Collaboration), Czech. J. Phys. **56**, F33 (2006).
[66] M. Anselmino, U. D'Alesio, S. Melis, and F. Murgia, Phys. Rev. D **74**, 094011 (2006).
[67] S. S. Adler *et al.* (PHENIX Collaboration), Phys. Rev. Lett. **95**, 202001 (2005).
[68] V. Barone, S. Melis, and A. Prokudin, Phys. Rev. D **81**, 114026 (2010).
[69] H. Gao *et al.*, Eur. Phys. J. Plus **126**, 1 (2011).